



The spectral sensitivity of the human short-wavelength sensitive cones derived from thresholds and color matches

Andrew Stockman ^{a,*}, Lindsay T. Sharpe ^b, Clemens Fach ^b

^a Department of Psychology, University of California San Diego, 9500 Gilman Drive, La Jolla, CA 92093-0109, USA

^b Forschungsstelle für Experimentelle Ophthalmologie, Röntgenweg 11, D-72076 Tübingen, Germany

Received 12 November 1997; received in revised form 30 March 1998

Abstract

We used two methods to estimate short-wave (S) cone spectral sensitivity. Firstly, we measured S-cone thresholds centrally and peripherally in five trichromats, and in three blue-cone monochromats, who lack functioning middle-wave (M) and long-wave (L) cones. Secondly, we analyzed standard color-matching data. Both methods yielded equivalent results, on the basis of which we propose new S-cone spectral sensitivity functions. At short and middle-wavelengths, our measurements are consistent with the color matching data of Stiles and Burch (1955, *Optica Acta*, 2, 168–181; 1959, *Optica Acta*, 6, 1–26), and other psychophysically measured functions, such as π_3 (Stiles, 1953, *Coloquio sobre problemas opticos de la vision*, 1, 65–103). At longer wavelengths, S-cone sensitivity has previously been over-estimated. © 1999 Elsevier Science Ltd. All rights reserved.

Keywords: S cones; Spectral sensitivity; Blue-cone monochromacy; Cone fundamental; Photopigment; Macular pigment; Lens pigment; Color matching

1. Introduction

The least abundant of the three cone photoreceptors are the short-wavelength-sensitive (S) cones. Absent in the very inner fovea, they never exceed a density of more than 10–15% of the total cone population in the central retina (1 deg eccentricity) nor more than 7–8% in the periphery (e.g. Stiles, 1949; Brindley, 1954; Wald, 1967; Williams, MacLeod & Hayhoe, 1981; Castano & Sperling, 1982; Ahnelt, Kolb & Pflug, 1987; Curcio, Allen, Sloan, Lerea, Hurley, Klock et al., 1991). Although they contribute comparatively little to our perception of spatial and temporal detail (e.g. Stiles, 1949; Brindley, 1954; Brindley, Du Croz & Rushton, 1966; Green, 1968; Kelly, 1974) and of luminance (e.g. Eisner & MacLeod, 1980 but see Stockman, MacLeod & De-

Priest, 1991), their spectral sensitivity provides the third dimension of normal trichromatic color vision.

Here, we quantify the S-cone spectral sensitivity in two ways: first by direct psychophysical measurements over a six log₁₀ unit sensitivity range in blue-cone monochromats and in normal observers; and second by analyzing existing color-matching data. We will consider each method in turn, as well as more direct measurements of S-cone spectral sensitivity.

1.1. Psychophysical measurements

Two principal psychophysical methods have been used to estimate S-cone spectral sensitivity in the normal observer: the test and field sensitivity methods (so-called by Stiles, 1978). In the test (or target) sensitivity method, an intense long-wavelength adapting field is presented to desensitize the L- and M-cones, so that the S-cones are more likely to mediate detection of a superimposed target. The sensitivity to the target is then measured as a function of target wavelength (e.g. Stiles, 1939, 1964; Wald, 1964). The suc-

* Corresponding author. Tel.: +1 619 5344762; fax: +1 619 5347190; e-mail astockman@ucsd.edu.

cess of this method depends on the extent to which the long-wavelength background field suppresses the M- and L-cones relative to the S-cones. Even with optimal backgrounds of high intensity, S-cone isolation in observers with normal color vision is generally not possible beyond ~ 540 nm (see Stiles, 1964; Wald, 1964; and below).

In the field sensitivity method, the background intensity that raises the threshold for a superimposed target by a criterion amount (usually one \log_{10} unit) is measured as a function of background wavelength (e.g. Stiles, 1939, 1946, 1953, 1959). For an S-cone-detected target, Stiles identified three mechanisms from his field sensitivity measurements, which he referred to as π_1 , π_2 and π_3 . Of these, the spectral sensitivity of π_3 is most like that of a photopigment, the other two having atypical, secondary sensitivity peaks at longer wavelengths. Yet, for the π_3 field sensitivity to be the spectral sensitivity of the S-cones, requires not only that the target be detected by only S-cones on background fields of all wavelengths, but also that those backgrounds raise S-cone threshold independently of their effects on the other cones. The requirement of independent S-cone adaptation becomes increasingly unlikely as the background wavelength increases, and backgrounds much more strongly excite the M- and L-cones than the S-cones.

In principle, the field sensitivity method has an advantage over the test sensitivity method in that it can be used to measure S-cone spectral sensitivity in normal observers to long wavelengths. In practice, however, the requirement of independent cone adaptation makes the validity of the field sensitivity method questionable. The test sensitivity method, which is not subject to the same requirement, since the background is fixed in intensity and wavelength, is, therefore, the preferred method. To make test sensitivity measurements throughout the spectrum, however, we must rely on a special type of observer—blue-cone (or S-cone) monochromats—who lack functioning M- and L-cones (see below) and, therefore obviate the problem of intrusion by other cones.

1.2. Analysis of color matching data

The color matching functions (CMFs) define the amounts of three primary lights—typically red, green and violet—that are required to match a series of monochromatic lights spanning the visible spectrum. Color matching data can be linearly transformed to other sets of real and imaginary primaries, including the ‘fundamental’ primaries, the color matching functions for which are the L-, M- and S-cone spectral sensitivities themselves.

Color matches are matches at the cone level. When matched, the test and mixture fields appear identical

to the S-cones, to the M-cones and to the L-cones. For a match between a mixture of the R, G and B primaries and the test field, λ , the following relationship applies:

$$\begin{pmatrix} \bar{l}_R & \bar{l}_G & \bar{l}_B \\ \bar{m}_R & \bar{m}_G & \bar{m}_B \\ 0 & \bar{s}_G & \bar{s}_B \end{pmatrix} \begin{pmatrix} \bar{r}(\lambda) \\ \bar{g}(\lambda) \\ \bar{b}(\lambda) \end{pmatrix} = \begin{pmatrix} \bar{l}(\lambda) \\ \bar{m}(\lambda) \\ \bar{s}(\lambda) \end{pmatrix}, \quad (1)$$

where $\bar{r}(\lambda)$, $\bar{g}(\lambda)$ and $\bar{b}(\lambda)$ are the red, green and blue CMFs, and $\bar{l}(\lambda)$, $\bar{m}(\lambda)$ and $\bar{s}(\lambda)$ (using a similar notation) are the L-, M- and S-cone spectral sensitivities or the fundamental CMFs (see Stockman & Sharpe, 1998). \bar{l}_R , \bar{l}_G and \bar{l}_B are, respectively, the L-cone sensitivities to the R, G and B primary lights, and similarly \bar{m}_R , \bar{m}_G and \bar{m}_B are the M-cone sensitivities to the primary lights, and \bar{s}_G and \bar{s}_B are the S-cone sensitivities (\bar{s}_R is effectively zero, if we assume, quite reasonably (see Table 3), that the S-cones are insensitive to the red primary). If we are concerned about only the relative cone spectral sensitivity, the transformation for $\bar{s}(\lambda)$ simplifies to:

$$(\bar{s}_G/\bar{s}_B)\bar{g}(\lambda) + \bar{b}(\lambda) = k_s \bar{s}(\lambda), \quad (2)$$

where k_s (or $1/\bar{s}_B$) is an unknown scaling constant (which we choose so that $\bar{s}(\lambda)$ has unity peak, see below), and where \bar{s}_G/\bar{s}_B is the value that we want to determine.

Eqs. (1) and (2) could be for an equal-energy or an equal-quanta spectrum. Since the CMFs are invariably tabulated for test lights of equal energy, we, like previous workers, use an energy spectrum to define \bar{s}_G/\bar{s}_B and to calculate the cone spectral sensitivities from the equal-energy CMFs. We then convert the relative cone spectral sensitivities from energy to quantal sensitivities (by multiplying by λ^{-1}). In general, when we consider the relationship of CMFs to cone spectral sensitivities we use energy units, and when we consider raw spectral sensitivity data or photopigment spectra, we use quantal units. The units are noted along the ordinate of the relevant figures. The tabulation of the cone spectral sensitivities in Table 3 is in quantal units.

Two methods can be used to determine \bar{s}_G/\bar{s}_B . The first method involves measuring S-cone spectral sensitivity directly, as outlined in Section 1.1, and then finding the linear combination of $\bar{b}(\lambda)$ and $\bar{g}(\lambda)$ that best describes it. The second method relies on the color matching data alone, which actually contain enough information to derive \bar{s}_G/\bar{s}_B without the need for other data (Bongard & Smirnov, 1954; Stockman, MacLeod & Johnson, 1993). The derivation is possible because the longer wavelength part of the visible spectrum is tritanopic (i.e. it effectively stimulates only the L- and M-cones). Test lights longer

than ~ 560 nm¹ are invisible to the S-cones at the radiances typically used to establish color matches, and can be matched for the M- and L-cones by a mixture of just the red and green primary lights. A small color difference typically remains, however, because the green primary light (but not the test light or red primary light) is seen by the S-cones. In order to complete the match for the S-cones, a small amount of the violet primary light must be added to the field opposite to the one containing the green primary. Since the sole purpose of the violet primary is to balance the quantal catch produced by the green primary in the S-cones, the ratio of the energies of the blue primary to green primary required for matches above ~ 560 nm should be constant and in inverse proportion to the S-cone spectral sensitivity to the two lights. The ratio equals \bar{s}_G/\bar{s}_B in Eq. (2). Put more formally, in the tritanopic region of the spectrum, Eq. (2) is equal to zero, so that:

$$-\frac{\bar{b}(\lambda)}{\bar{g}(\lambda)} = \frac{\bar{s}_G}{\bar{s}_B}. \quad (3)$$

Once \bar{s}_G/\bar{s}_B is known, the S-cone spectral sensitivity function can be calculated by combining $\bar{g}(\lambda)$ and $\bar{b}(\lambda)$ according to Eq. (2). A limitation of this calculation is that it defines S-cone sensitivity only over the spectral range over which the S-cones contribute to the detection of the monochromatic test light (i.e. to ~ 560 nm, after which the ratio of the energies of the blue to green primaries becomes constant).

The validity of S-cone spectral sensitivities, derived directly from color matches, depends crucially on the accuracy of the matching data in the middle- and long-wavelength region. Unfortunately, much of the data in this region has been adjusted to correct for rod intrusion or to simplify the data. The data of Guild (1931, Table II), for example, on which the CIE 1931 2 deg CMFs are partly based, were adjusted by making the violet CMF equal to zero at wavelengths longer than 630 nm (see below), thereby distorting the color matching data and eliminating information about the S-cone spectral sensitivity.

¹ The exact wavelength at which the test light becomes invisible to the S-cones depends on the intensity at which the matches are carried out, and on the S-cone sensitivity of the subject. It is characterized by the ratio of violet to green CMFs becoming constant. The absolute S-cone sensitivity for a 560 nm target can be estimated roughly from Stiles' model of the π -mechanisms (see Table 1(7.4.1) and Table 2(7.4.3) and Sections 7.4.2 and 7.4.3 of Wyszecki & Stiles, 1982a). The peak sensitivity of π_1 is ~ 6.5 log quanta s^{-1} deg⁻² at 444.4 nm. Thus, from our Table 3, column 1a, the sensitivity at 560 nm (ignoring the difference in target size) should be ~ 9.7 log quanta s^{-1} deg⁻² (or 3.6 log ph td). Stiles and Burch (1955) carried out their 2° matches near 560 nm with a target of between 2.6 and 3.2 log ph. td, while Stiles and Burch (1959) carried out their 10° color matches with a target of 2.8 or 3.5 log ph. td. For both target sizes, the test field should be below S-cone threshold.

Remarkably, most estimates of S-cone spectral sensitivity that are defined as linear combinations of CMFs are actually inconsistent with the color matching data on which they are based. That is, they are inconsistent with the ratio of \bar{s}_G/\bar{s}_B implied by the color matching data in the tritanopic region. These issues will be discussed further below.

1.3. Direct measures

Relevant direct measures of S-cone spectral sensitivity include microspectrophotometric measurements in humans (Dartnall, Bowmaker & Mollon, 1983). Such estimates can be compared with corneally-measured S-cone spectral sensitivities, once the latter have been corrected to the photoreceptor level by removing the effects of the lens and macular pigments, and then adjusting them to a low photopigment optical density. To ensure that the appropriate corrections were made, we estimated the macular, lens and peak photopigment optical densities of each of our observers (see below).

Another direct measure is spectral sensitivity data obtained from suction electrode recordings of single cone photoreceptors. So far, however, data are available only for macaque monkey S-cones, which have a longer λ_{\max} than human S-cones.

Also of relevance in this context are theoretical 'standard' photopigment template shapes, such as the template recently proposed by Lamb (1995). The Lamb template is supposed to characterize the shapes of all photopigment spectra when they are plotted on a log wavelength, log frequency or normalized frequency scale (all of which are equivalent). It can be used to evaluate the plausibility of S-cone photopigment spectra derived from psychophysical measurements. One limitation of the Lamb template is that it characterizes the photopigment spectrum well only near the λ_{\max} and at wavelengths longer than the λ_{\max} , but this limitation is less of a concern for S-cone measurements, which typically end at wavelengths only 30 or 40 nm below the S-cone λ_{\max} .

1.4. Blue-cone monochromats

Blue-cone monochromats (or S-cone monochromats) were first described by Blackwell and Blackwell (1957; 1961), who concluded that they had rods and S-cones, but lacked M- and L-cones. Though two studies suggested that blue-cone monochromats might also possess a second cone type containing the rod photopigment (Pokorny, Smith & Swartley, 1970; Alpern, Lee, Maa-seidvaag & Miller, 1971), subsequent studies have supported the original conclusion of Blackwell & Blackwell that they have only rods and S-cones (Daw & Enoch, 1973; Hess, Mullen, Sharpe & Zrenner, 1989).

Pedigree studies show that blue-cone monochromacy is an X-linked recessive trait (e.g. Falls, 1960; Spivey,

1965). A molecular genetic analysis of the M- and L-cone photopigment gene array on the X-chromosome of blue-cone monochromats shows that the deficit can arise for a number of different reasons, including deletions, or loss of function due to homologous recombination and point mutation (Nathans, Davenport, Maunene, Lewis, Hejtmancik, Litt et al., 1989; Nathans, Maunene, Zrenner, Sadowski, Sharpe, Lewis et al., 1993).

Spectral sensitivities in ‘classic’ blue-cone monochromats have been measured several times before (e.g. Blackwell & Blackwell, 1961; Grütznert, 1964; Alpern, Lee & Spivey, 1965; Alpern et al., 1971; Daw & Enoch, 1973; Smith, Pokorny, Delleman, Cozijnsen, Houtman & Went, 1983, (patient V-4); Hess et al., 1989), and are typical of the S-cones. A concern about the use of blue-cone monochromats to obtain a standard S-cone spectral sensitivity for central vision, however, is that they usually fixate extrafoveally (but there are exceptions, see Hess et al., 1989). Consequently, in order to use blue-cone monochromats to estimate normal S-cone spectral sensitivity, it is necessary to estimate their macular and photopigment optical densities, and, if necessary, correct them to normal density values. Moreover, some individuals in pedigrees with blue-cone monochromacy reveal residual L-cone function if large or even small test fields are used (cf. Smith et al., 1983). Thus, caution must be exercised when selecting candidates, whose genotypes should be known.

2. Objectives

The principal objective of this project was to define the S-cone spectral sensitivity of normal human color vision. Two methods were used. First, we measured S-cone test sensitivities in five normal trichromats and in three blue-cone monochromats of known genotype—over as large a spectral range as possible with our apparatus, and using a fine spectral interval. Secondly, we analyzed existing color matching data.

On the basis of the new work, we define the S-cone spectral sensitivity at short- and middle-wavelengths as a linear transformation of the $\bar{g}(\lambda)$ and $\bar{b}(\lambda)$ CMFs (i.e. we find the value of \bar{s}_G/\bar{s}_B in Eq. (2)). At longer wavelengths, after which the CMFs no longer define the S-cone spectral sensitivity, we rely primarily on our threshold measurements.

A secondary objective of this project was to estimate the macular, lens and photopigment optical densities of each observer, and to identify the underlying causes of the individual differences between the S-cone spectral sensitivities. To this end, we measured S-cone test sensitivities both centrally and peripherally to yield estimates of each observer’s macular pigment and photopigment optical densities, and made supplementary scotopic

measurements to provide an estimate of each observer’s lens density. The photopigment template of Lamb (1995), which agreed well with our individual and group spectral sensitivities, provided a means of estimating the underlying λ_{\max} values.

3. General methods

3.1. Subjects

Five male color normal observers (AS, CF, HJ, LS, and TA) and three male blue-cone monochromats (FB, KS and PS) were used in these experiments.

The three blue-cone monochromats are known to lack M- and L-cone function on both behavioral and genetic grounds. PS has been an observer in several psychophysical studies (Zrenner, Magnussen & Lorenz, 1988; Hess et al., 1989; Reitner, Sharpe & Zrenner, 1991; Sharpe, Fach & Stockman, 1992), and KS and FB have been observers in one previous study (Reitner et al., 1991). All three were part of the Nathans et al. (1993) molecular genetic study of 33 subjects with ‘blue-cone monochromacy or closely related variants of blue-cone monochromacy’. Observer PS has two X-chromosome photopigment genes but has an upstream deletion in the region that controls their expression. Observers KS and FB have a single X-chromosome photopigment gene with a point mutation that results in a Cys to Arg substitution at position 203 in the opsin (Nathans et al., 1993). An upstream deletion was found in six of the 33 subjects of the Nathans et al. study, and a C203R point mutation was found in 16.

The blue-cone monochromats may on average fixate slightly extrafoveally. Hess et al. (1989) report that PS has a 2 deg vertically eccentric fixation in the superior retina (see their Fig. 1B). KS fixates temporally slightly above the fovea (Zrenner, personal communication). Our own measurements indicate that PS fixates 3 deg superior to the retina and FB fixates 1–2 deg temporal to the retina. To be able to correct for the effects of extrafoveal fixation, we estimated the macular pigment and photopigment optical densities in our observers.

3.2. Apparatus

The optical apparatus was a conventional Maxwellian-view optical system that produced 2 mm diameter output beams at the pupil. Each channel was made up of four achromatic lenses, and other standard optical components, such as mirrors and beamsplitters. A 75 W Xenon arc lamp illuminated the target field, while a 100 W Mercury arc lamp illuminated the background field. Test and field stimuli were defined by circular field stops. The position of the observer’s head was maintained by a dental wax impression.

Infra-red radiation was minimized by heat absorbing glass placed early in each beam. Fixed neutral density filters were added as required. Variable neutral density wedges were positioned in the beams, mounted on computer-controlled stepping motors.

3.3. Stimuli

The test target was 2 deg in diameter and was presented in the center of a 16 deg diameter background field. Target wavelengths were selected by a computer-controlled Jobin Yvon H-10 monochromator with 0.5 mm slits. The spectral output of the monochromator was a triangular function of wavelength with a bandwidth at half maximum output (the ‘full width at half maximum’ or FWHM) of 4 nm. At wavelengths above 560 nm, a Schott OG550 cut-off filter was added to attenuate the short wavelength (< 550 nm) part of the small skirt of scattered light leaked by the monochromator (see below). We produced continuous 1 Hz square-wave flicker using a mechanical shutter driven by a function generator.

Field wavelengths were selected by the use of 3-cavity, blocked interference filters with FWHMs of between 7 and 11 nm. For the five normals, a 12.10 log quanta $s^{-1} \text{ deg}^{-2}$ (5.90 log photopic td), 580 nm background was used. This background was chosen to desensitize the L and M-cones, while having relatively little effect on the S-cones. The use of a shorter wavelength background would have reduced S-cone sensitivity, whereas the use of a longer wavelength one would have spared the M-cones. For the three blue-cone monochromats, an 11.24 log quanta $s^{-1} \text{ deg}^{-2}$, 620 nm background was used. This background (3.36 log scotopic td or 4.68 log photopic td) was chosen to ensure rod saturation, but to have a minimal effect on the S-cones. The 12.10 log quanta $s^{-1} \text{ deg}^{-2}$, 580 nm background was not used for the blue-cone monochromats, because it is intense enough to raise S-cone threshold directly (for the S-cones, the 580 nm field is equivalent to a 440 nm field of 8.02 log quanta $s^{-1} \text{ deg}^{-2}$; see Function 1a of Table 3). Its use would have restricted the range of wavelengths over which S-cone sensitivity could be measured.

Spectral sensitivities were obtained centrally and at an eccentricity of 13 deg in the temporal retina. Fixation was maintained with the aid of a small fixation light. The differences between the central and peripheral measurements were analyzed to provide an estimate of the macular density.

In the scotopic spectral sensitivity measurements, which were carried out to estimate lens pigment densities (see below), a dim 620 nm background of 6.25 log quanta $s^{-1} \text{ deg}^{-2}$ (-1.63 log scotopic td or -0.31 log photopic td) was used.

3.4. Calibration

The radiant fluxes of test and background fields were measured at the plane of the observers’ pupil with a radiometer (UDT). The calibration of the UDT radiometer was checked against a similar model (now produced by Graseby), both of which had been calibrated by the manufacturers against standards traceable to the National Bureau of Standards, Washington. In addition, the UDT radiometer was checked against a photodiode that was calibrated against the German national standard. All three instruments gave consistent measurements.

Neutral density filters, fixed and variable, were calibrated *in situ* for all test and field wavelengths used. Particular care was taken in calibrating the monochromator and interference filters: a spectroradiometer (Spectrascan, Photoresarch) was used to measure the center wavelength and FWHM at each wavelength setting of the monochromator. With 0.5 mm slits, the FWHM of the test lights produced by the Jobin Yvon H-10 monochromator was 4 nm. The stray light rejection more than 8 nm away from the selected wavelength was $\sim 10^{-5}$. For most experiments, such a skirt of stray light would be unimportant. In spectral sensitivity measurements, however, the skirt becomes critical when the sensitivity to the target wavelength falls far below the maximum sensitivity. At such wavelengths, the light at the entrance to the monochromator has to be made so bright to be detected that the subject may detect the skirt as well as (or instead of) the target wavelength. At 610 nm, for example, the S-cone sensitivity is about $10^{-5.5}$ less than at 440 nm, so that the blue-cone

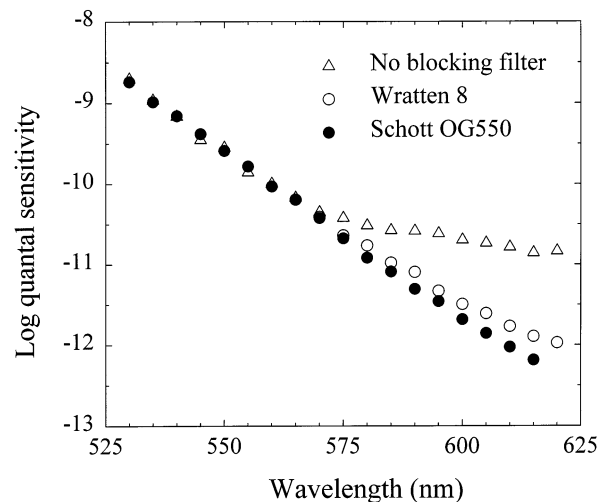


Fig. 1. Spectral sensitivity curves measured in a blue-cone monochromat (PS) with no blocking filter in the test channel (open triangles), with a Wratten 8 gelatin filter (open circles) and with a Schott OG550 glass filter (filled circles). Deviations above the function denoted by the filled circles are due to the detection of the skirt of stray light transmitted by the Jobin-Yvon H-10 monochromator.

monochromat detects the skirt rather than the 610 nm target (see Fig. 1). To reduce the skirt, we added a glass cut-off filter (a Schott OG550) that blocked short wavelengths, but transmitted wavelengths longer than 550 nm.

The skirt produced by the monochromator was so small that it was difficult to measure with conventional calibration devices such as spectroradiometers or photometers. We found that the most efficient device with which to check for the presence of the skirt was the human, blue-cone monochromat observer. The effect of the skirt is simple to calculate, and easy to see in the measured spectral sensitivity curve. Fig. 1 shows spectral sensitivity curves measured in a blue-cone monochromat (PS) with no blocking filter in the test channel (open triangles), with a Wratten 8 gelatin filter (open circles) and with a Schott OG550 glass filter (filled circles).

With no blocking filters present (open triangles), the skirt causes the sensitivity to deviate from the assumed S-cone spectral sensitivity at ~ 560 nm and to reach a shallow plateau. With a Wratten #8 blocking filter present (open circles), which cuts off 50% of the light by ~ 495 nm and $> 10^{-3}$ below 460 nm, the deviation is smaller and begins at ~ 585 nm. With a Schott OG550 filter present (filled circles), which cuts off 50% of light by ~ 550 nm and $> 10^{-5}$ below 530 nm, the spectral sensitivity curve reaches an asymptotic shape. That is, the shape of the spectral sensitivity curve measured with a Schott OG550 filter did not change with the addition of further blocking filters, which suggests that it represents the observer's true spectral sensitivity.

3.5. Spectral sensitivity determinations

In the main experimental runs, target wavelengths were randomly varied in 5 nm steps from either 390 or 400 nm to either 570 nm for normals or 580 nm for blue-cone monochromats. On each trial, subjects adjusted the intensity of the flickering light until they were satisfied that the flicker was just at threshold. Five threshold settings were made at each target wavelength. After each setting, the intensity of the flickering light was randomly reset to either a higher or a lower intensity, so that the subject had to readjust the intensity to find threshold. Four complete runs were carried out by each subject with central presentation of the target and four with peripheral presentation. Each data point, therefore, represents twenty threshold settings.

In the secondary runs for the blue-cone monochromats, target wavelengths were randomly varied in 5 nm steps from 560 to 615 nm. An additional OG550 blocking filter was added to eliminate the effects of the skirt transmitted by the monochromator (see above). Again, five settings were made at each wavelength during each of four separate runs. At 620 nm, there was insufficient light for the subjects to set the threshold consistently.

For normals, who showed evidence of M- or L-cone intrusion by ~ 540 nm, target wavelengths were varied from 540 to 650 nm in 10 nm steps. Since these measurements were not used to define spectral sensitivity, only two runs were carried out.

3.6. Subjective target color

The marked difference in the slopes of the S-cone and of the M- and L-cone spectral sensitivity functions at middle-wavelengths (Stockman et al., 1993) suggests that a change from target detection by the S-cones to target detection by the M- or L-cones should cause an abrupt change in the slope of the spectral sensitivity curve (see Fig. 2a, below). The transition, however, may be obscured by interactions between the S and the M- or L-cones, when more than one cone type detects the target.

As a check on the range of cone isolation, we noted, in a separate experiment, how the appearance of the near-threshold target depended on target wavelength. If only the S-cones detect the target, its appearance should not change with wavelength. This was the case for the blue-cone monochromats: over the entire spectral region measured, they reported no change in appearance. In the normals, however, the appearance changed after ~ 540 nm. Importantly, the color change coincided closely with the change in the slope of the normals' spectral sensitivity curves. Though not conclusive, since an achromatic mechanism with more than one cone input could also give an unchanging percept, this type of evidence is strongly suggestive in the case of the S-cones, which are thought to feed predominantly into chromatic channels (e.g. Mollon, 1982).

3.7. Individual variability

Two important sources of variability in the shapes of measured cone spectral sensitivities are individual differences in the densities of lens and macular pigmentation. These prereceptor filters absorb mostly at short-wavelengths and so affect S-cone spectral sensitivity measurements near the S-cone λ_{\max} . Individual differences can be large: in studies using more than ten subjects, macular pigment density has been found to vary from 0.0 to 1.2 at 460 nm (Wald, 1945; Bone & Sparrock, 1971; Pease, Adams & Nuccio, 1987), and lens pigment density by approximately 25% of the mean density implied by the $V'(\lambda)$ function (see van Norren & Vos, 1974). We estimated the macular and lens densities in each of our subjects, as well as a third lesser source of variability, photopigment optical density.

3.7.1. Lens pigment density

Lens pigment densities were estimated from 1 Hz rod thresholds measured at test wavelengths of 400, 420, 460

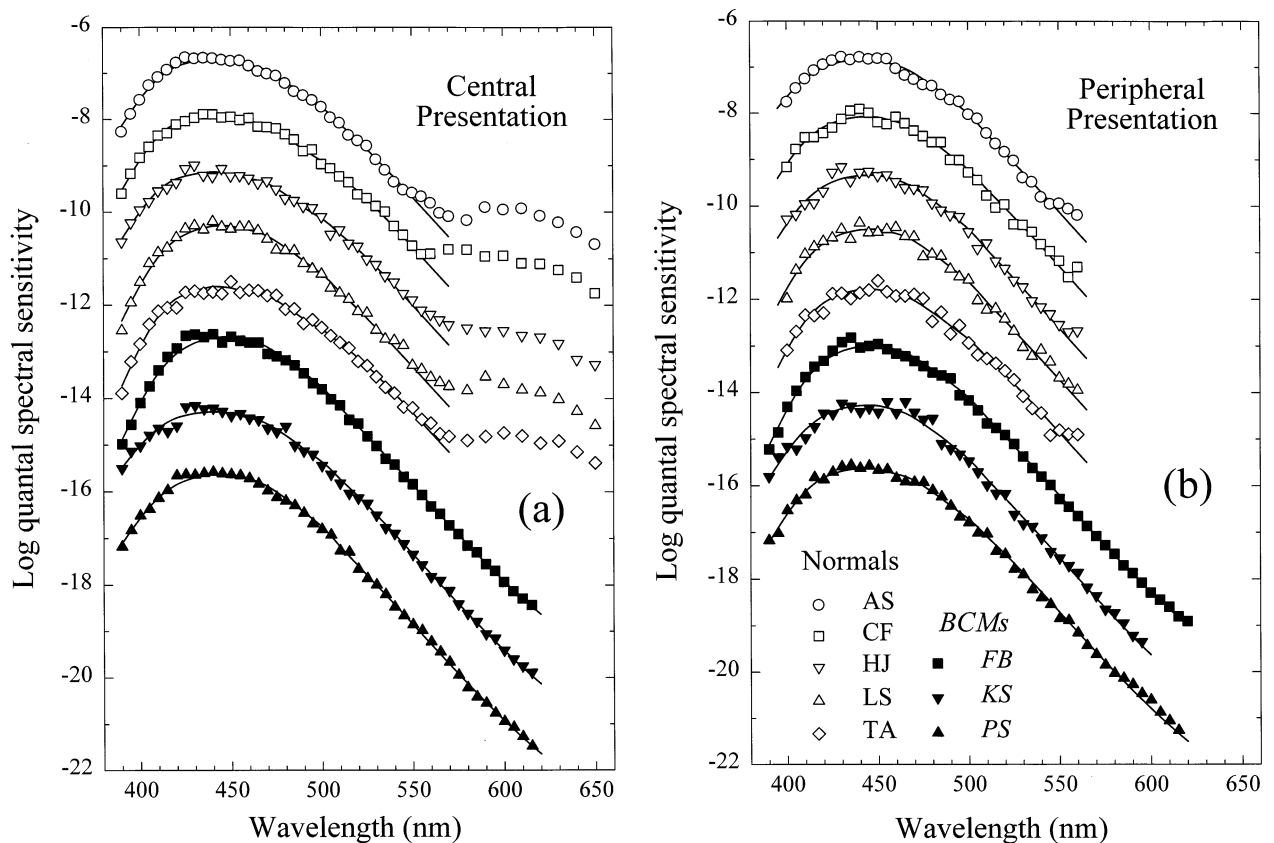


Fig. 2. (a) Individual 1 Hz spectral sensitivities obtained with central presentation. Each data set, except that for AS, has been displaced vertically for clarity: by -1.2 (CF), -2.0 (HJ), -3.8 (LS), -4.0 (TA), -6.3 (FB), -8.1 (KS) and -9.7 (PS) log units. Open symbols denote observers with normal color vision: AS (circles), CF (squares), HJ (inverted triangles), LS (triangles) and TA (diamonds). Filled symbols denote blue-cone monochromats: FB (squares), KS (inverted triangles) and PS (triangles). The same key is used throughout to identify each subject's data. Continuous lines show the proposed 2 deg S-cone spectral sensitivity function (Function 1a, Table 3) individually adjusted in macular and lens densities to fit each data set. (b) Individual 1 Hz spectral sensitivities obtained at 13 deg in the temporal retina. Each data set, except that for AS, has been displaced vertically: by -1.0 (CF), -2.2 (HJ), -4.0 (LS), -4.3 (TA), -6.5 (FB), -7.2 (KS) and -9.1 (PS) log units. Continuous lines show the proposed 10 deg S-cone spectral sensitivity function (Function 1b, Table 3) individually adjusted in macular and lens densities to fit each data set. Other details as (a).

and 500 nm at an eccentricity of 13 deg in the temporal retina by comparing them with the corresponding values of the standard $V'(\lambda)$ scotopic luminosity function (Table I (4.3.2) of Wyszecki & Stiles, 1982a). We assumed that differences between the shape of $V'(\lambda)$ and the rod functions for each individual subject reflect lens absorption in the violet (essentially the method of Ruddock, 1965). This assumption neglects individual differences in the optical density of rhodopsin between observers, but such effects are relatively minor compared with the much larger effects that can be caused by variations in lens density. Each set of rod spectral sensitivity measurements was preceded by 40 min of dark adaptation. A dim 620 nm background of $6.25 \log \text{ quanta s}^{-1} \text{ deg}^{-2}$ ($-1.63 \log \text{ sc td}$ or $-0.31 \log \text{ ph td}$) was used, mainly to aid fixation. The scotopic spectral sensitivities were averaged from twenty settings: four separate runs of five threshold settings per target wavelength.

To estimate the density, we assumed the lens density spectrum tabulated in Table 3 of the Appendix. We also

allowed a vertical shift of the log spectral sensitivity curves in order to account for wavelength-independent changes in overall sensitivity between subjects. With the use of a standard curve-fitting algorithm (the Marquardt-Levenberg algorithm, implemented in SigmaPlot, Jandel Scientific, San Rafael, CA), we found: (1) the value by which the lens density spectrum should be multiplied before being added to or subtracted from each subject's data and (2) the vertical shift that together with (1) minimized the squared deviations between the subject's data and $V'(\lambda)$. This estimate of lens density yields the relative difference in density between each of our subjects and the mean density of the 50 observers upon which the $V'(\lambda)$ function was based. Arbitrarily, we report lens densities relative to the tabulated template.

A relative estimate of the differences in lens density between our subjects can also be obtained from the differences between the S-cone spectral sensitivities. Since macular pigment, the other principle source of variability, is absent at 13 deg in the periphery (e.g. Bone,

Landrum, Fernandez & Tarsis, 1988, Table 2 and p. 847), we used the peripheral measurements to estimate the lens density differences. We used a similar method to that used to estimate lens density differences from the rod measurements, except that we minimized the squared deviations between the subject's data and the mean data for all subjects (rather than $V'(\lambda)$). Such an analysis ignores individual variability in the peripheral S-cone photopigment optical density, the effects of which are comparatively small (see below). This estimate of lens density yields the relative difference in density between each subject and the mean density for all eight subjects.

We found that the lens density estimates obtained from the rod and S-cone spectral sensitivity estimates agreed fairly well, with the exception of one subject (FB), whose rod measurements were suspect (see below).

3.7.2. Macular pigment and photopigment densities

We estimated macular pigment and photopigment densities by comparing the 1 Hz flicker spectral sensitivities measured centrally with those measured at an eccentricity of 13 deg. Since macular pigment is absent by 13 deg eccentricity, the macular density estimate is the absolute macular density for a 2 deg, centrally-presented target. The photopigment optical density estimate is, however, a relative measure.

Two estimates were carried out for each subject. First, we ignored the changes in photopigment optical density with eccentricity, and accounted for the differences in shape between the central and peripheral spectral sensitivity curves solely in terms of a change in macular pigment. We assumed the macular density spectrum tabulated in Table 3 of the Appendix, which is based on measurements provided by Bone (personal communication), and allowed a vertical shift in log sensitivity between the central and peripheral data. Such a shift is necessary because subjects are more sensitive to the target when it is presented centrally than when it is presented at 13 deg in the periphery. With the use of a standard curve-fitting algorithm, we found: (1) the factor by which the macular density spectrum should be multiplied before being added to each subject's central data and (2) the vertical shift that together with (1) minimized the squared deviations between the subject's central and peripheral data. Several other studies have estimated macular pigment density by isolating the same cone mechanism in the fovea and periphery in this way (e.g. Stiles, 1953).

In the second estimate, we accounted for the differences in shape between the central and peripheral spectral sensitivity curves in terms of changes in macular pigment density and photopigment density. We used the same procedure as before, except that we also allowed the axial peak optical density (D_{peak}) to vary in

making the fits. The effect of varying D_{peak} on the shape of the quantal spectral sensitivity curve at the retina ($J(\lambda)$) can be calculated with the use of the following standard formula (see Knowles & Dartnall, 1977, p. 56):

$$J(\lambda) = 1 - 10^{-D_{\text{peak}}A(\lambda)}, \quad (4)$$

where $A(\lambda)$ is the absorbance spectrum of the photopigment normalized to unity peak. The application of this formula requires that the quantal spectral sensitivity at the retina ($J(\lambda)$) be calculated from the (measured) quantal corneal spectral sensitivities. To make this calculation, we used the lens density values obtained from rod spectral sensitivity measurements (see above). In addition, we needed to adopt a value for the peak optical density of the photopigment at 13 deg in the periphery. Within limits, this choice has a minimal effect on the estimate of the change in density in going from the center to 13 deg in the periphery. We assumed a value of 0.20.

We adopted the template based on the data provided by Bone (see Table 3) in preference to other templates, because its use in the above analysis yielded plausible estimates of the S-cone photopigment optical density change from the central to the peripheral retina. In contrast, the Vos (1972) and Wyszecki and Stiles (1982a) templates yielded estimates of the optical density change that were implausibly high (see below). The differences between the templates are mainly at very short wavelengths, where the reliability of the Vos, and Wyszecki & Stiles templates is questionable.

4. Results

4.1. Psychophysical measurements of spectral sensitivity

Fig. 2a shows the individual 1 Hz spectral sensitivities for all eight subjects obtained with central presentation. Each data set, except the highest one, has been displaced vertically for clarity. The upper five sets (open symbols) are those for the normal observers (AS, CF, HJ, LS and TA) measured on the 12.10 log quanta $\text{s}^{-1} \text{deg}^{-2}$, 580 nm background. The lower three sets (filled symbols) are those for the blue-cone monochromats (FB, KS and PS) measured on the 11.24 log quanta $\text{s}^{-1} \text{deg}^{-2}$, 620 nm background. The continuous lines drawn through each set of data are the proposed 2 deg S-cone spectral sensitivity function (Function 1a, Table 3) optimally adjusted in macular and lens densities to fit each data set.

The curves in Fig. 2a are all reasonably similar in shape from 390 to ~ 540 nm, which suggests the operation of a photoreceptor (or other mechanism) common to all subjects. After ~ 540 nm, however, the curves for the normals and blue-cone monochromats

diverge. In the normals, the divergence is accompanied by a clear change in the apparent color of the target field and an apparent sharpening of its borders. In contrast, the blue-cone monochromats saw no change in the appearance of the target throughout the spectrum. The differences between the groups are consistent with the M- and L-cones taking over target detection above ~ 540 nm in normals, but not in the blue-cone monochromats.

Fig. 2b shows the individual 1 Hz spectral sensitivities for all eight subjects measured peripherally. Again the data sets have been displaced vertically for clarity. Peripheral data for normals were measured from 400 to 560 nm, and for blue-cone monochromats from 390 to 615 nm, except for KS, who was relatively insensitive in the periphery, and ran out of light at 600 nm. Up to ~ 540 nm, the results for the two groups are again fairly similar, after which they begin to diverge. As with the central measurements, there is no evidence of M- and L-cone involvement in the spectral sensitivity data for the blue-cone monochromats. The continuous lines drawn through each data set are the proposed 10 deg S-cone spectral sensitivity function (Function 1b, Table 3) optimally adjusted in macular and lens densities. (While the S-cone photopigment optical density for the 13 deg peripheral measurements is probably slightly lower than that for a 10 deg field, the 10 deg S-cone functions describe the peripheral data well.)

To emphasize the differences between individual spectral sensitivity data, we have superimposed the central and peripheral data from 390 to 560 nm in Fig. 3 (a,c), respectively. Each subject's data has been shifted vertically to minimize the squared deviations (from 390 to 540 nm) between the subject's data and the mean for all observers. Fig. 3 (b,d) show the differences between each individual's data and the mean for the central and peripheral measurements, respectively.

While the overall differences are relatively small over most of the spectral range, there are clear individual differences in both the central (Fig. 3a,b) and the peripheral (Fig. 3c,d) measurements. The differences at short-wavelengths are likely to be caused by individual variation in the densities of lens and macular pigmentation. There are, however, also differences at longer wavelengths. In particular, the central data for the blue-cone monochromats (filled symbols) tend to fall slightly more steeply than those for normals (open symbols) in the range 440–530 nm. As we argue below, this steepening is probably due to a lower photopigment optical density in the blue-cone monochromat observers, who, in contrast to normal observers, do not fixate centrally.

Next, we estimated the macular, lens and photopigment densities of each of the observers, and used those values to try to account for the individual differences between the S-cone spectral sensitivities.

4.2. Lens pigment density

Rod spectral sensitivities (not shown) were measured at target wavelengths of 400, 420, 460 and 500 nm on a dim 620 nm background of $6.25 \log \text{ quanta s}^{-1} \text{ deg}^{-2}$.

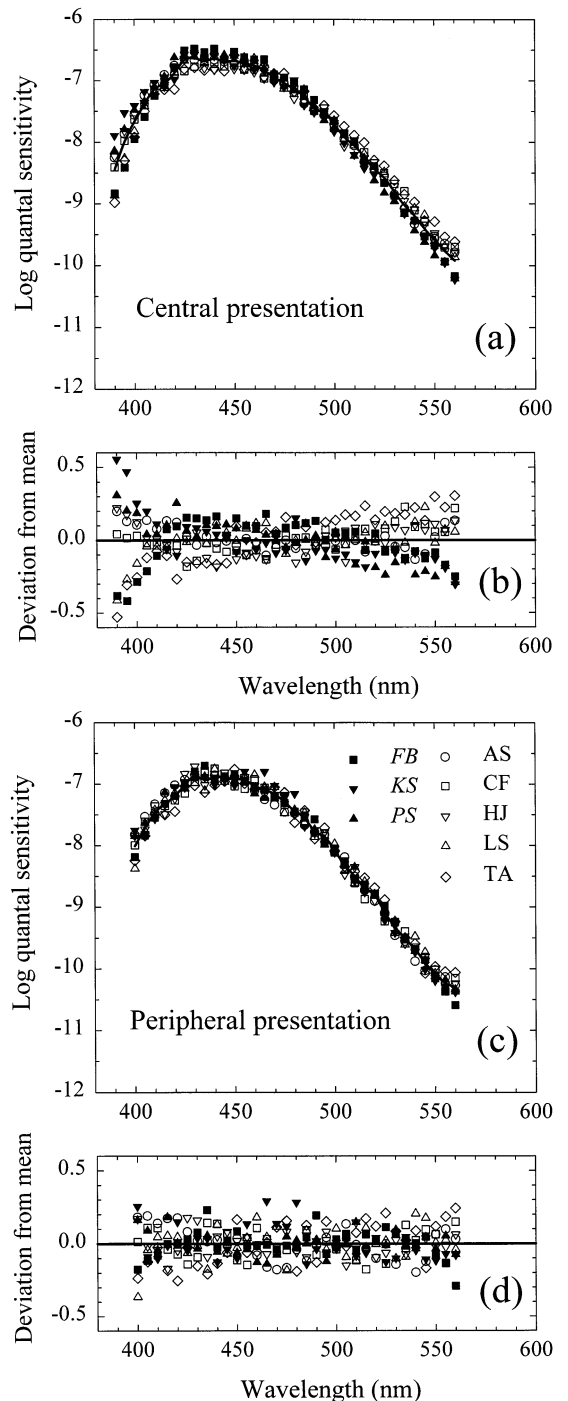


Fig. 3. Upper panels: Individual central (a) and peripheral (c) spectral sensitivities from 390 to 560 nm (symbols) shifted vertically to align with the mean function (continuous lines). Lower panels: Residual differences between the shifted and mean data for (b) central and (d) peripheral presentation.

Table 1
Lens density estimates

Subjects	Scotopic measurements			S-cone peripheral measurements		
	Relative lens density	Shift	rms error	Relative lens density	Shift	rms error
AS	-0.08 ± 0.09	-0.11 ± 0.08	0.07	-0.18 ± 0.04	-0.01 ± 0.02	0.08
CF	-0.06 ± 0.13	-0.08 ± 0.12	0.12	-0.03 ± 0.05	0.17 ± 0.02	0.10
HJ	-0.12 ± 0.01	-0.06 ± 0.01	0.01	-0.04 ± 0.04	0.26 ± 0.02	0.08
LS	0.15 ± 0.07	-0.33 ± 0.06	0.06	0.11 ± 0.05	-0.43 ± 0.03	0.11
TA	0.20 ± 0.06	0.26 ± 0.05	0.05	0.21 ± 0.06	0.53 ± 0.03	0.12
FB	0.08 ± 0.05	—	—	0.08 ± 0.05	-0.40 ± 0.02	0.09
KS	-0.08 ± 0.05	0.73 ± 0.05	0.05	-0.07 ± 0.06	0.27 ± 0.03	0.11
PS	-0.06 ± 0.08	-0.41 ± 0.07	0.06	-0.08 ± 0.03	-0.39 ± 0.02	0.07
Normals	0.02	-0.06		0.02	0.10	
BCMs	-0.02	0.16		-0.02	-0.17	
All	0.00	0.00		0.00	0.00	

Lens density estimates. Subjects: Initials indicate normal observers (AS, CF, HJ, LS and TA) or blue-cone monochromats (FB, KS, PS). Normals, BCMs (blue-cone monochromats) and All indicate group averages. Scotopic measurements: Adjustments in lens density (Column 2) and logarithmic vertical shifts (Column 3) required to bring each subject's rod spectral sensitivities into best agreement with the scotopic $V'(\lambda)$ function, and the residual root-mean-squared (rms) errors (Column 4). The lens density adjustments are the best-fitting values. The adjustments are tabulated relative to the mean adjustment for all subjects, which was 0.09. Our observers, therefore, have, on average, 0.09 times less lens density than the observers on which the scotopic $V'(\lambda)$ function is based. (The value for FB is from the S-cone measurements.) S-cone peripheral measurements: Adjustments in lens density (Column 5) and logarithmic vertical shifts (Column 6) required to bring each subject's peripheral S-cone spectral sensitivity into best agreement with the mean function for all observers, and the residual rms errors (Column 7). The lens density adjustments are relative to the lens density spectrum tabulated in Table 3 of the Appendix. Specifically, the values in Columns 2 and 5 are the values by which the lens spectrum is multiplied before being added to the individual spectral sensitivity data to bring them into best agreement with the mean spectral sensitivity data. The values preceded by the symbol \pm are the estimated standard errors of each fitted parameter.

As outlined in the Methods section, we determined the adjustment in lens density and the vertical shift that together minimized the squared deviations between the subject's data and $V'(\lambda)$. These values are tabulated in Table 1 relative to the mean adjustment for all subjects. They are the values by which the lens template in Table 3 is multiplied before being added to (if the subject has more lens pigment than average) or subtracted from (if the subject has less lens pigment than average) his rod spectral sensitivity data. The range of lens densities adjustments (Column 2) is from 0.20 (i.e. 0.20 more lens density than average) to -0.12 , and the mean is 0.00. The average adjustment relative to the scotopic $V'(\lambda)$ was -0.09 , which implies that our observers have 0.09 less lens density than the observers on which $V'(\lambda)$ is based. The vertical shifts (Column 3) range from -0.33 to 0.73. (The absolute shifts relative to $V'(\lambda)$ are arbitrary, since $V'(\lambda)$ is normalized to unity peak.) We were unable to obtain a plausible rod spectral sensitivity from FB, and, unfortunately, unable to make repeat measurements.

A secondary estimate of lens pigment density was derived from the differences between the peripheral S-cone spectral sensitivities. As described above, we determined the increase or decrease in lens density and the vertical shift that together minimized the squared deviations between each subject's spectral sensitivity and the mean S-cone data for all subjects. The results are given in Columns 5–7. Except for AS and HJ, the changes in lens densities (Column 5) are in good agree-

ment with the those derived from the rod spectral sensitivities. In the remaining calculations, we adopted the lens densities estimated from the rod measurements, except for FB, for whom we adopted the lens density estimates based on the S-cone measurements. On the basis of calculations of photopigment spectra from individual and mean corneal spectral sensitivities (see, for example, Fig. 13) and other considerations, we assume that the mean lens density of our observers is 85% of the standard lens density spectrum given in Table 3 of the Appendix.

4.3. Macular pigment and photopigment densities

Macular pigment and photopigment densities both decline with eccentricity, with the former becoming negligible after ~ 10 deg of eccentricity. We estimated the decline in both by comparing the S-cone spectral sensitivities measured centrally and peripherally (see above).

First, though, we ignored changes in photopigment optical density with eccentricity and found the macular density and the vertical shift that minimized the squared deviations between each subject's central and peripheral data. These values are tabulated in Columns 2 and 3 of Table 2. Macular densities at 460 nm (Column 2) vary from 0.48 to -0.06 with a mean density of 0.21. Consistent with their suspected extrafoveal fixation, the blue-cone monochromats have a low mean macular density of only 0.09, whereas the

Table 2
Macular density estimates

Subjects	Without photopigment optical density adjustments			With photopigment optical density adjustments			
	Macular density at 460 nm	Shift	rms error	Macular density at 460 nm	Change in pigment density	Shift	rms error
AS	0.17 ± 0.05	0.30 ± 0.04	0.06	0.18 ± 0.04	0.26 ± 0.06	0.25 ± 0.03	0.04
CF	0.21 ± 0.09	0.58 ± 0.06	0.10	0.20 ± 0.07	0.26 ± 0.07	0.54 ± 0.05	0.08
HJ	0.48 ± 0.06	0.41 ± 0.04	0.09	0.41 ± 0.05	0.20 ± 0.04	0.34 ± 0.03	0.06
LS	0.23 ± 0.08	0.19 ± 0.05	0.09	0.22 ± 0.06	0.25 ± 0.09	0.14 ± 0.05	0.08
TA	0.32 ± 0.07	0.22 ± 0.05	0.10	0.30 ± 0.05	0.19 ± 0.05	0.20 ± 0.04	0.07
FB	0.02 ± 0.05	0.04 ± 0.03	0.08	−0.02 ± 0.05	0.15 ± 0.07	−0.01 ± 0.04	0.08
KS	0.31 ± 0.08	1.21 ± 0.07	0.14	0.31 ± 0.09	−0.01 ± 0.16	1.22 ± 0.08	0.14
PS	−0.06 ± 0.06	0.54 ± 0.04	0.10	−0.06 ± 0.06	−0.04 ± 0.07	0.56 ± 0.05	0.10
Normals	0.28	0.38		0.26	0.23	0.29	
BCMs	0.09	0.60		0.08	0.03	0.59	
All	0.21	0.47		0.19	0.16	0.41	

Subjects: Initials indicate normal observers (AS, CF, HJ, LS and TA) or blue-cone monochromats (FB, KS, PS). Normals, BCMS (blue-cone monochromats) and All indicate group averages. Without photopigment optical density adjustments: reductions in macular density (Column 2) and vertical logarithmic shifts (Column 3) required to bring each subject's central S-cone spectral sensitivities into best agreement with his peripheral S-cone spectral sensitivities, and the rms errors of the fit (Column 4). The macular density is given as the density at 460 nm, which is near the peak of the macular density spectrum (see below). With photopigment optical density adjustments: Reductions in macular density (Column 5), photopigment density (Column 6) and vertical logarithmic shifts (Column 7) required to bring each subject's central S-cone spectral sensitivities into best agreement with his peripheral S-cone spectral sensitivities, and the rms errors of the fit (Column 8).

We assumed the macular and lens density spectra tabulated in the Table 3. The values preceded by the symbol ± are the estimated standard errors of each fitted parameter.

normals have a higher mean density of 0.28. The normal subjects have comparable macular densities for a 2 deg field to the 11 subjects of Stockman et al. (1993), for whom the average density was 0.32. Vertical shifts in Column 3 vary from 1.21 to 0.04 with a mean of 0.47.

Fig. 4a illustrates how well macular pigment accounts for the differences between the central and peripheral data for the five normal observers. The continuous line is the macular pigment spectrum based on data from Bone (personal communication) from Table 3, scaled to a peak value of 0.28. The dotted circles are the mean differences between the peripheral and central measurements. Before averaging, each individual's data were vertically shifted in accordance with Column 3 of Table 2, and then scaled to the mean peak macular density of 0.28. We show only the mean, scaled differences for normals. The macular densities for PS and FB are too low to be useful in determining the macular spectrum, and the data for KS were too noisy.

If macular pigment alone accounts for the differences in shape between the central and peripheral measurements, then the dotted circles and continuous line shown in Fig. 4a should coincide. However, the data fall above the template at wavelengths shorter than ~450 nm and below it at longer wavelengths. These discrepancies could be the result of a decline in photopigment optical density with eccentricity.

Accordingly, in the second fit, we found the photopigment optical density difference, the macular den-

sity and the vertical shift that minimized the squared deviations between each subject's central and peripheral data. The results are tabulated in Columns 5–8 of Table 2. Changes in peak photopigment optical density (Column 6) vary from 0.26 to −0.04 with a mean change of 0.16. However, the values for two groups differ markedly: the mean value for the normals is 0.23, while that for the blue-cone monochromats is 0.03. Macular densities at 460 nm (Column 5) vary from 0.41 to −0.06 with a mean density of 0.19. Again, the mean value of 0.08 for the blue-cone monochromats is much lower than the mean value of 0.26 for the normals. The vertical shifts (Column 7) vary from 1.22 to −0.01.

This analysis suggests that the blue-cone monochromats fixate extrafoveally. Both FB and PS have a slightly negative difference in macular density (KS is in the normal range), and all three have low photopigment density differences. The slightly negative values for the macular density changes in PS and FB and the photopigment optical density changes in PS do not differ significantly from zero. The results for PS, which yield negative values for both density estimates, suggest that his fixation may have been such that the stimuli fell slightly closer to the fovea with 'peripheral' than with 'central' presentation (as would be the case if his fixation were, for example, 7 deg in the nasal retina). According to Hess et al. (1989) and our own measurements, however, PS has a vertically eccentric fixation of only 2–3 deg in the superior retina (see their Fig. 1B), which argues against such an interpretation.

Fig. 4b is similar to Fig. 4a, except that the difference between each observer's central and peripheral data have been vertically shifted (Column 7) and corrected for the difference in photopigment density (Column 6), before being scaled to the mean peak macular density for normals of 0.26. In this case, the continuous line is the macular pigment spectrum scaled to a peak value of 0.26. Again, we show only mean, scaled differences for the normals. After the adjustment for changes in photopigment density with eccentricity, the means agree better with the macular density spectrum.

Comparisons between the mean group data show that the peripheral spectral sensitivities for both the normals and the blue-cone monochromats and the central spectral sensitivities for the blue-cone monochromats all have similarly low photopigment optical densities. Only the central spectral sensitivities for the normals have the higher photopigment density as indicated in Table 2. Thus, our group of blue-cone monochromats have close to normal photopigment optical densities with peripheral presentation of the target, but abnormally low densities with central presentation.

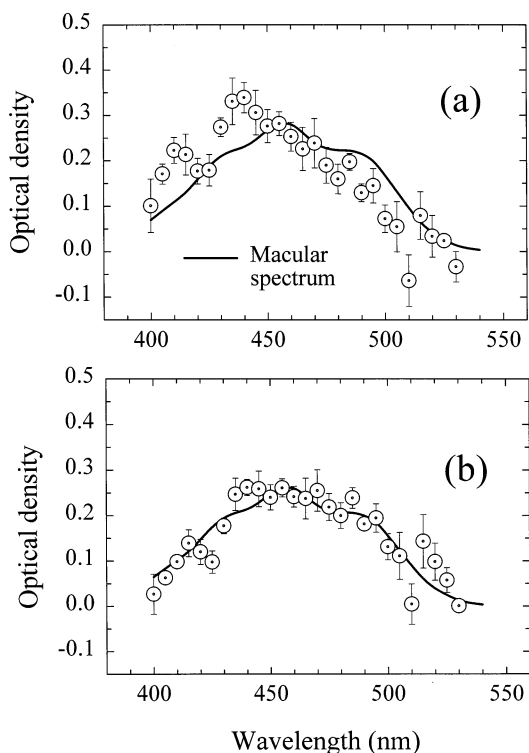


Fig. 4. Mean relative differences between the peripheral and central S-cone spectral sensitivity functions after the differences for each subject were scaled for consistency with a peak macular density of 0.28 (a) or 0.26 (b). Differences (dotted symbols) are shown with (a) no adjustments and (b) optimal adjustments in photopigment optical density between the central and peripheral functions (see text and Table 2 for details). The errors bars in all figures, if shown, are ± 1 standard error. Continuous lines are the macular density spectrum from Table 3 scaled to scaled to peak at 0.28 (a) or 0.26 (b). Data for normals only.

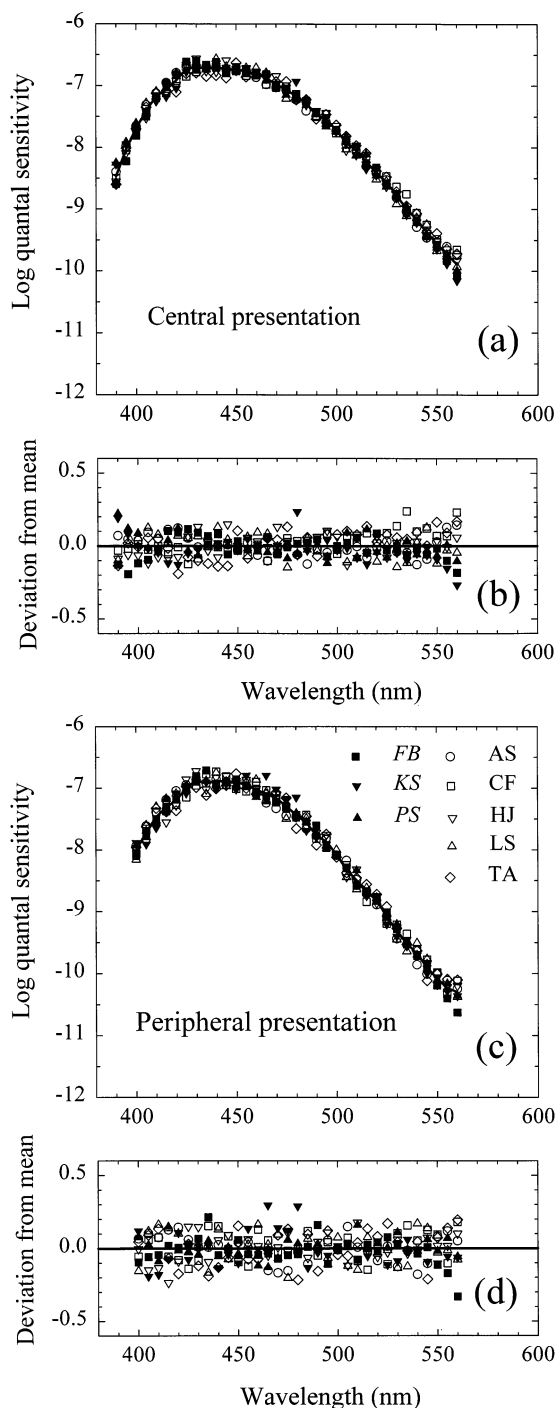


Fig. 5. Individual central (a) and peripheral (b) spectral sensitivities from 390 to 560 nm (symbols) corrected to mean density values and shifted vertically to align with the mean spectral sensitivity functions (continuous lines). The individual central functions (a) were corrected to the mean lens densities for all subjects, and to the mean macular and photopigment densities for the normal subjects. The individual peripheral functions (b) were corrected to the mean lens densities for all subjects.

Fig. 5 shows again the central and peripheral data. This figure is similar to Fig. 3, but now the individual data in Fig. 5a have been corrected to the mean lens,

and mean normal macular and photopigment densities, while in Fig. 5b they have been corrected to the mean lens density. In both panels, the individual data have been vertically shifted to align with the mean function for all observers. The data now agree remarkably well except above 540 nm, after which the other cones take over target detection in the normals. The small deviations below 400 nm suggest small errors in some of the lens pigment density estimates.

4.4. Average S-cone spectral sensitivity functions

To produce the final central average from 390 to 540 nm, we individually corrected the blue-cone monochromat spectral sensitivity data to the mean normal macular and photopigment densities and averaged them with the unadjusted normal spectral sensitivity data. We made individual adjustments only to the central blue-cone monochromat spectral sensitivities, for which there was good evidence that the optical and macular density values lay outside normal range. No other data were adjusted.

To produce the final peripheral average from 400 to 540 nm, we simply averaged together the individual spectral sensitivity data from both groups. We made no adjustments to the individual data before averaging, since there was no reason to suppose that the individual density values for any of the normal or blue-cone monochromat observers lay outside the normal range.

While our analysis suggests that most of the individual densities lie within the normal range, it also suggests that the mean lens and macular densities will be lower than the normal population means. Thus, it is likely that the mean spectral sensitivities will have to be adjusted to higher macular and lens densities for consistency with other S-cone estimates. This expectation is borne out in the comparisons below.

Fig. 6 illustrates how the long-wavelength blue-cone monochromat data (open symbols) were combined with the mean data (filled symbols) outside the spectral range of the normal measurements. We took advantage of the finding that the \log_{10} S-cone spectral sensitivity versus wavelength functions of the blue-cone monochromat observers from 520 to 615 nm are well described by a straight line (see Fig. 6). We used a standard curve-fitting algorithm to find the slope and intercept of the straight line that best described the blue-cone monochromat data from 530 to 615 nm and all the data from 520 to 540 nm. As part of the fit, the blue-cone monochromat data were allowed to shift vertically. The results are shown in Fig. 6. The aligned data sets were averaged in their overlapping region and combined. An unexpected result was that the peripheral data (squares) fall slightly less steeply with wavelength than the central data (circles). The slopes of the lines shown in Fig. 6 are -0.0386 for the peripheral data

and -0.0412 for the central data. The difference could be due to noise, but it might also reflect differences in the size and structure of the central and peripheral photoreceptors and thus their interactions with light.

4.5. Average S-cone spectral sensitivities and standard color matching functions

We next found the linear combinations of the standard 2 deg $\bar{b}(\lambda)$ and $\bar{g}(\lambda)$ CMFs that best describe our average psychophysical data with and without adjustments to the macular and lens densities. For a central 2 deg field, the two primary determinations of the CMFs are the 1955 Stiles and Burch $\bar{r}(\lambda)$, $\bar{g}(\lambda)$ and $\bar{b}(\lambda)$ CMFs and the Judd, Vos modified 1931 CIE $\bar{r}(\lambda)$, $\bar{g}(\lambda)$ and $\bar{b}(\lambda)$ CMFs (and their transform, the CIE $\bar{x}(\lambda)$, $\bar{y}(\lambda)$ and $\bar{z}(\lambda)$ CMFs). We will consider each set in turn.

If our psychophysical data truly represent the S-cone spectral sensitivity, then they should be describable as linear combinations of the CMFs. Moreover, the results should agree with the linear combinations derived directly from the color matching data in the next section. Macular and lens density adjustments are required because the densities of the mean observer in the color matching experiments are unlikely to correspond precisely to the densities of the mean observer used in our study.

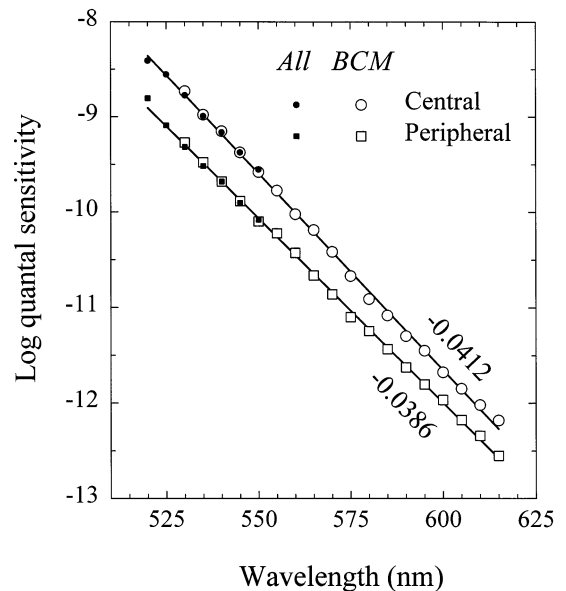


Fig. 6. Alignment of the long-wavelength blue-cone monochromat data (open symbols) with the mean data for all subjects (filled symbols) for the central (circles) and peripheral (squares) measurements. The straight lines are those that best describe both the mean data from 520 to 540 nm and the blue-cone monochromat data from 530 to 615 nm. As part of the fit, the blue-cone monochromat data were allowed to shift vertically to the positions shown in the figure. The lines have slopes of -0.0412 (central data) and -0.0386 (peripheral data).

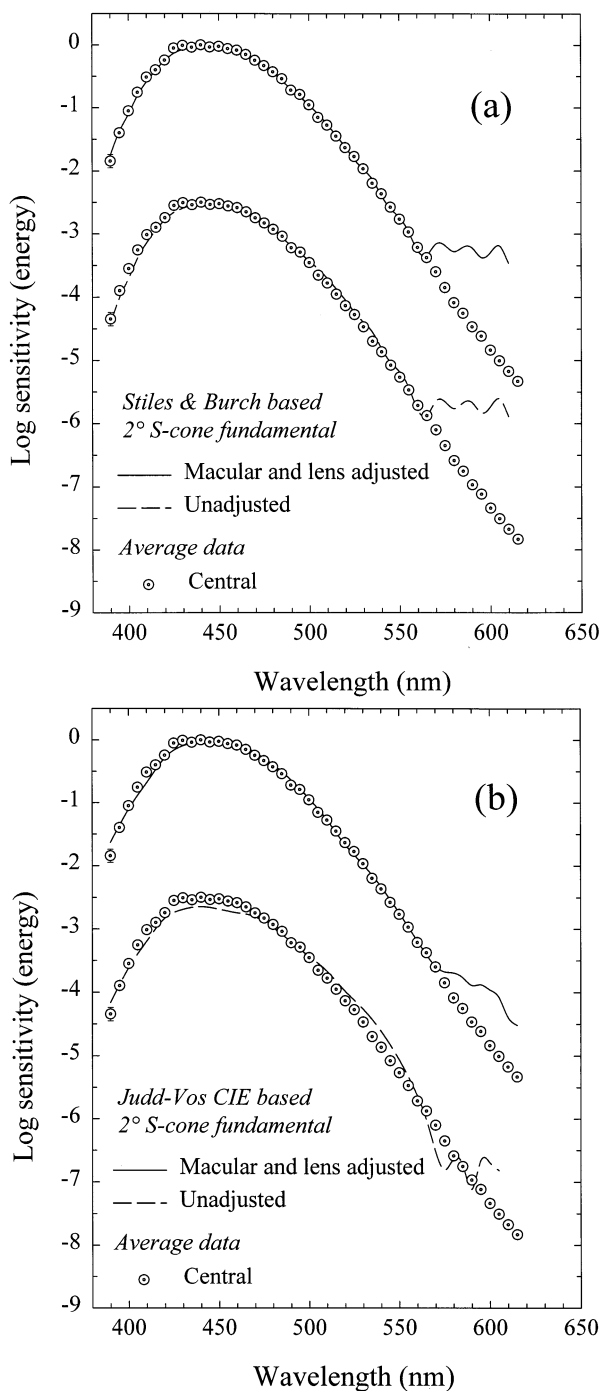


Fig. 7. (a) Linear combinations of the Stiles and Burch (1955) 2 deg $\bar{b}(\lambda)$ and $\bar{g}(\lambda)$ CMFs that best fit (≤ 565 nm) the mean central data (dotted circles) with $(\bar{b}(\lambda) + 0.01630\bar{g}(\lambda))$, continuous line, upper function) or without $(\bar{b}(\lambda) + 0.01613\bar{g}(\lambda))$, dashed line, lower function) adjustments in lens and macular pigment density. The two fits are separated vertically for clarity. (b) Linear combinations of the CIE Judd, Vos 2 deg $\bar{b}(\lambda)$ and $\bar{g}(\lambda)$ CMFs that best fit (≤ 565 nm) the mean central data (dotted circles) with $(\bar{b}(\lambda) + 0.0087\bar{g}(\lambda))$, continuous line, upper function) or without $(\bar{b}(\lambda) + 0.0079\bar{g}(\lambda))$, dashed line, lower function) adjustments in lens and macular pigment density.

Fig. 7 a shows the mean central data for our subjects twice (dotted circles), with the two instances vertically separated for clarity by 2.5 log units, and the upper instance normalized to peak at zero. The linear combinations of the Stiles and Burch 2 deg $\bar{b}(\lambda)$ and $\bar{g}(\lambda)$ CMFs that best fit the data (≤ 565 nm) with (continuous line, upper functions) or without (dashed line, lower functions) adjustments in lens and macular pigment density. Both uncorrected $(\bar{b}(\lambda) + 0.01613\bar{g}(\lambda))$ and corrected $(\bar{b}(\lambda) + 0.01630\bar{g}(\lambda))$ fits are fairly good, but the fit with macular and lens adjustments is excellent up to 565 nm. In the upper fit, in which macular and lens densities were allowed to vary, our subjects have 0.09 less lens pigment (i.e. in terms of the lens density template of Table 3, their densities are 10% of the template lower) and a peak macular density of 0.06 less than the Stiles and Burch 2 deg observer. The root-mean-squared (rms) errors ≤ 565 nm were 0.039 with macular and lens density adjustments and 0.068 without adjustments. Since we use equal-energy CMFs, the spectral sensitivity data in this figure are in energy units.

Fig. 7b shows the linear combinations of the CIE Judd, Vos 2 deg $\bar{b}(\lambda)$ and $\bar{g}(\lambda)$ CMFs that best fit the data (≤ 565 nm) with (continuous line) or without (dashed line) corrections to account for differences in lens and macular pigment density. The fit without macular and lens adjustments $(\bar{b}(\lambda) + 0.0079\bar{g}(\lambda))$ is poor throughout the spectrum, but the relative weights agree with those implied by ratio of the $b(\lambda)$ to $g(\lambda)$ chromaticity coordinates (see Fig. 8a). In contrast, the fit with macular and lens adjustments $(\bar{b}(\lambda) + 0.0087\bar{g}(\lambda))$ is reasonably good except at short-wavelengths (e.g. 400–430 nm). According to this fit, our subjects have 0.09 less lens pigment (relative to the lens pigment density template) and a peak macular density of 0.42 less than the CIE Judd, Vos 2 deg observer. However, the suggested macular adjustment is implausible, since it implies that the mean CIE Judd, Vos observer had a peak macular density of more than 0.63, which is nearly twice the expected density for a 2 deg field (see p. 2496 of Stockman et al., 1993). The rms errors ≤ 565 nm were 0.066 with macular and lens density adjustments and 0.143 without adjustments. For comparison, the best fits of the Smith and Pokorny S-cone fundamental ($\bar{e}(\lambda)$) to the experimental data ≤ 565 nm have rms errors of 0.080 with macular and lens density adjustments and 0.200 without adjustments.

If the seemingly high macular densities of the average CIE Judd, Vos observer were actually due to macular pigment, a straightforward correction could bring those CMFs into the normal range (e.g. Smith, Pokorny & Zaidi, 1983). Unfortunately, the high macular densities implied by the Judd, Vos CIE CMFs are not due to macular pigment *per se*. They arise because of adjustments that were made by Judd (1951) to the 1931 CMFs in an attempt to overcome errors in the original

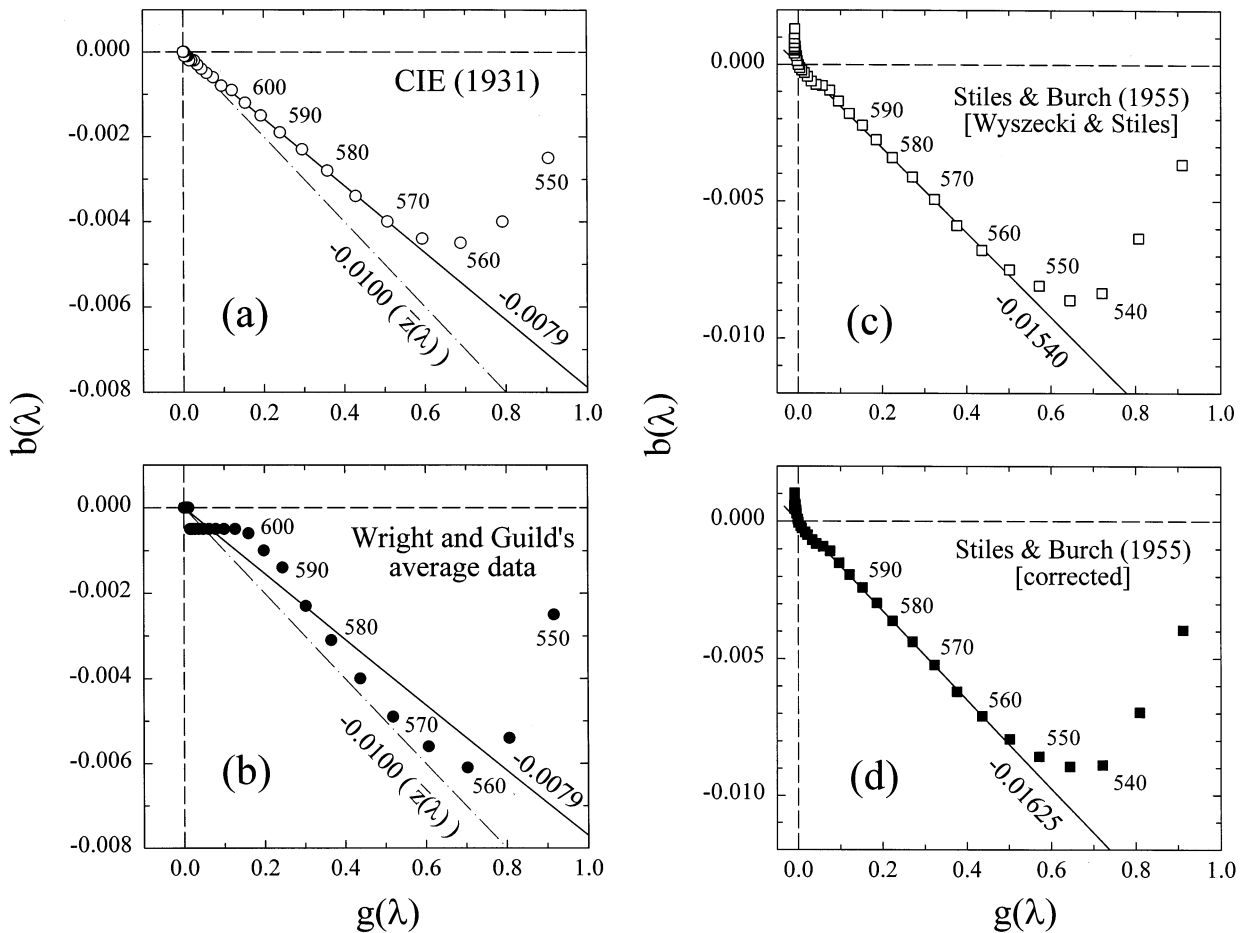


Fig. 8. (a) CIE 1931 2 deg $g(\lambda)$ chromaticity coordinates plotted against the $b(\lambda)$ chromaticity coordinates (open circles). The best-fitting line from 565 to 600 nm (solid line) has a slope of -0.0079 . The $\bar{z}(\lambda)$ CMF (and Smith & Pokorny S-cone fundamental) implies the dot-dashed lines in panels (a) and (b) with a slope of -0.0100 . (b) Mean Wright (1928–29) and Guild (1931) 2 deg $g(\lambda)$ plotted against $b(\lambda)$ (filled circles). The best-fitting line from 565 to 600 nm (solid line) has a slope of -0.0079 . (c) Versions of Stiles and Burch (1955) $g(\lambda)$ chromaticity coordinates plotted against the $b(\lambda)$ chromaticity coordinates (open squares) from Table I (5.5.3) of Wyszecki and Stiles (1982a). The best-fitting straight line from 555 nm to long-wavelengths (continuous line) has a slope of -0.01540 . (d) Versions of Stiles and Burch (1955) $g(\lambda)$ chromaticity coordinates plotted against the $b(\lambda)$ chromaticity coordinates (filled squares) corrected according to the instructions in Stiles and Burch (1959). The best-fitting straight line from 555 nm to long-wavelengths (continuous line) has a slope of -0.01625 . (The more familiar plot of chromaticity coordinates is $r(\lambda)$ versus $g(\lambda)$).

1924 CIE $V(\lambda)$ function, which is too insensitive at short-wavelengths. However, since Judd restricted his adjustments to wavelengths shorter than 460 nm (the peak of the macular density spectrum), when the corrections could have been extended to still longer wavelengths, he produced an observer with an artificially high macular pigment density (see Stockman et al., 1993).

Aside from the problems with the CIE color matching data at short wavelengths, the results of our analysis show that the S-cone fundamental ($\bar{b}(\lambda) + 0.0100\bar{g}(\lambda)$) or $\bar{z}(\lambda)$, which was proposed by Wyszecki and Stiles (1967), by Vos and Walraven (1971) and by Smith and Pokorny (1975), is not the optimal one in the CIE space. A weight of 0.0087 or lower on $\bar{g}(\lambda)$ is more consistent with the color matching data.

4.6. S-cone spectral sensitivities directly from color matching data

As explained in the introduction, it is also possible to derive the central S-cone spectral sensitivity functions directly from color matching data. We will consider the 1931 CIE $\bar{r}(\lambda)$, $\bar{g}(\lambda)$ and $\bar{b}(\lambda)$ CMFs and then the 1955 Stiles & Burch $\bar{r}(\lambda)$, $\bar{g}(\lambda)$ and $\bar{b}(\lambda)$ CMFs.

The usefulness of the 1931 CIE CMFs and variants thereof is, unfortunately, limited. Rather than being measured directly, they were constructed from the mean chromaticity coordinates of Wright (1928–29) and Guild (1931) with the assumption that the CMFs must be a linear combination of the 1924 CIE $V(\lambda)$ curve. Not only is the validity of the $V(\lambda)$ curve, even after the corrections of Judd and Vos have been applied questionable (see Stockman et al., 1993) but so too is the

assumption that $V(\lambda)$ must be a linear combination of the CMFs (Sperling, 1958; Estévez, 1979). There are other problems, however, which can be traced back to the original color matching data on which the CIE 1931 functions are based, and to the ways in which the original data were ‘corrected’ before being adopted by the CIE. These problems are particularly relevant to any derivation of the S-cone spectral sensitivity using the CIE 1931 data.

Fig. 8a shows as open circles the 1931 CIE $g(\lambda)$ chromaticity coordinate plotted against the $b(\lambda)$ chromaticity coordinate at middle- and long-wavelengths. (The $b(\lambda)$ chromaticity coordinate is $\bar{b}(\lambda)/(\bar{r}(\lambda) + \bar{g}(\lambda) + \bar{b}(\lambda))$ and the $g(\lambda)$ chromaticity coordinate is $\bar{g}(\lambda)/(\bar{r}(\lambda) + \bar{g}(\lambda) + \bar{b}(\lambda))$). As expected, the function is close to a straight line from 565 to 600 nm. The slope of the best-fitting line (continuous line) over this range is -0.0079 , which, as discussed above, implies that the relative S-cone spectral sensitivity is $\bar{b}(\lambda) + 0.0079\bar{g}(\lambda)$.

The $\bar{z}(\lambda)$ CMF (or $\bar{b}(\lambda) + 0.0100\bar{g}(\lambda)$), which has been adopted by many as their S-cone spectral sensitivity estimate (e.g. Wyszecki & Stiles, 1969; Vos & Walraven, 1971; Smith & Pokorny, 1975), implies the dot-dashed line shown in Fig. 8a (and 8b) with a slope of -0.0100 . Not only does this line entirely avoid the chromaticity data, but the resulting fundamental (Fig. 11a, filled circles) deviates implausibly from a photopigment spectrum after 545 nm. The function that maintains a plausible shape over the greatest spectral range is $\bar{b}(\lambda) + 0.0087\bar{g}(\lambda)$ (Fig. 7b, continuous line). It diverges from our data after ~ 570 nm, after which the CMFs no longer usefully define the S-cone spectral sensitivity, because longer test wavelengths at the radiances typically used in color-matching determinations are invisible to the S-cones.

The CIE chromaticity data of Fig. 8a are idealized versions of the original data of Wright (1928–29) and Guild (1931) on which they are based. Fig. 8b (filled circles) shows the mean $g(\lambda)$ versus $b(\lambda)$ chromaticity coordinates of Wright (1928–29) and Guild (1931) averaged by Guild (1931, Table III). This plot of $g(\lambda)$ versus $b(\lambda)$ follows, as expected, a straight line from 550 to ~ 600 nm. Unexpectedly, though, this straight line does not pass through the origin. (The CIE’s correction to these data is indicated by the solid line with a slope of -0.0079 , while the dot-dashed line with a slope of -0.0100 is the line implied by $\bar{z}(\lambda)$). A problem associated with the averaged Wright and Guild data can be traced back to the original chromaticity coordinates of Guild (1931, Table II). Unfortunately, Guild arbitrarily fixed the blue chromaticity to zero above 630 nm, when, in fact, it should have crossed the origin and changed sign. This simplification of his data, once transformed to the CIE primaries, gives rise to the distortion seen in Fig. 8b. It would be possible to correct the original data of Guild, retrans-

form them to the original primaries, and then recalculate the CIE functions. But there seems to be little point in perpetuating a system of colorimetry that is fundamentally flawed, and for which a better alternative exists.

We can avoid the problems associated with the 1931 CIE data by using instead the Stiles and Burch (1955) CMFs, which were directly measured rather than being reconstructed from chromaticity data. Fig. 8c (open squares) shows the Stiles and Burch $g(\lambda)$ chromaticity coordinate plotted against the $b(\lambda)$ chromaticity coordinate at middle- and long-wavelengths. The color matching data are from Table I (5.5.3) of Wyszecki and Stiles (1982a). Like the CIE data, and in accordance with our model, the function is close to a straight line from 555 nm to long-wavelengths. The best-fitting line (continuous line) has a slope of -0.01540 , which implies that the S-cone fundamental is $\bar{b}(\lambda) + 0.01540\bar{g}(\lambda)$. Surprisingly, though, this function (not shown) deviates from a plausible photopigment spectrum and the psychophysical data after 535 nm.

If, instead of the Stiles & Burch functions tabulated in Wyszecki and Stiles (1982a), we use the original data (corrected according to instructions in Stiles & Burch (1959) for a calibration error), we obtain the function shown in Fig. 8d (filled squares), which is fitted by a straight line (continuous line) with a slope of -0.1625 . The resulting S-cone fundamental ($\bar{b}(\lambda) + 0.01625\bar{g}(\lambda)$), which is similar to the function $\bar{b}(\lambda) + 0.01630\bar{g}(\lambda)$ shown as the continuous line in Fig. 7a, agrees well with the psychophysical data up to 565 nm. In terms of the original Stiles and Burch 2 deg color matching data, then, our preferred S-cone fundamental is $\bar{b}(\lambda) + 0.01625\bar{g}(\lambda)$. This deviates only slightly from the function ($\bar{b}(\lambda) + 0.01650\bar{g}(\lambda)$) suggested by Stockman et al. (1993).

The reason for the small differences between the original version and the Wyszecki and Stiles version of the Stiles and Burch (1955) CMFs is unclear. Both make corrections for the calibration error noted in Stiles and Burch (1959) and transform the data to the same primaries. However, our analysis suggests that of the two, only the original version retains the correct ratio of $b(\lambda)$ to $g(\lambda)$ at middle- and long-wavelengths. It is reassuring that the solution ($\bar{b}(\lambda) + 0.01630\bar{g}(\lambda)$) obtained from the present psychophysical measurements (see Fig. 7a) agrees to three significant figures with the solution derived directly from the original Stiles and Burch (1955) color matching data ($\bar{b}(\lambda) + 0.01625\bar{g}(\lambda)$).

We note that the corrections applied to the CIE and to the Stiles and Burch 2 deg color matching data are in a region where the $\bar{b}(\lambda)$ CMF is so small that the adjustments were probably considered, incorrectly it now turns out, to be unimportant.

5. Discussion

Based on spectral sensitivity measurements in five normal observers and three blue-cone monochromats, we propose the S-cone fundamentals tabulated in Table 3 of the Appendix. The versions are based on: (1a,b) the Stiles and Burch (1959) 10 deg CMFs corrected to 2 deg (Function 1a, Table 3) and uncorrected (Function 1b, Table 3); (2) the Stiles and Burch (1955) 2 deg CMFs (Function 2, Table 3); and (3) the 2 deg CIE 1931 CMFs corrected by Judd (Judd, 1951) and Vos (1978) (Function 3, Table 3). The three 2 deg fundamentals are illustrated in Fig. 9 (continuous lines).

Of these, we prefer functions 1a and 1b, since they are based on the extensive 10 deg color matching measurements of Stiles and Burch (1959), which form the main basis of the CIE 1964 10 deg functions. Moreover, the two functions provide a consistent fundamental for both 2 deg (small-field) and 10 deg (large-field) vision. Function 2 is provided for comparison, but is based on the 2 deg ‘pilot’ data of Stiles and

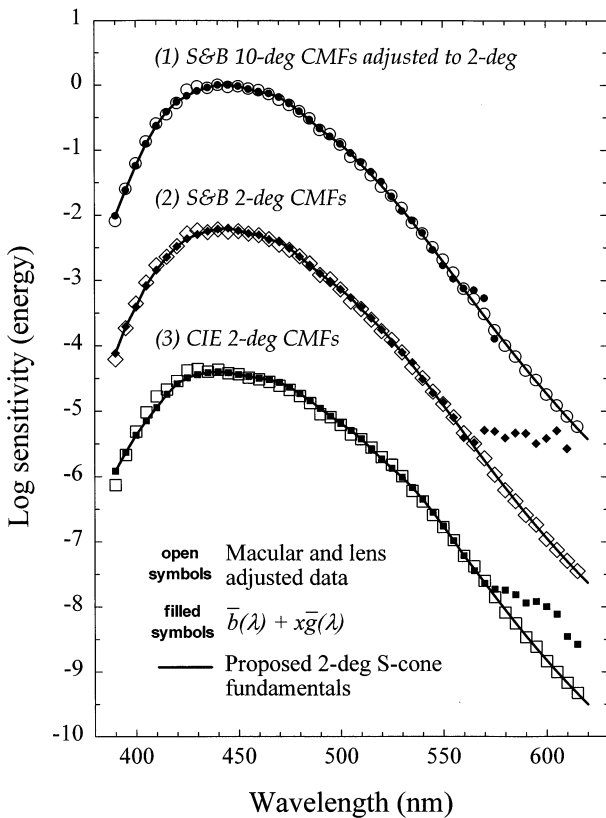


Fig. 9. Proposed cone fundamentals (continuous lines) based on (1) the Stiles and Burch (1959) 10 deg CMFs corrected to 2 deg; (2) the Stiles and Burch (1955) 2 deg CMFs and (3) the 2 deg CIE 1931 CMFs corrected by Judd (1951) and Vos (1978). Filled symbols: $\bar{b}(\lambda) + x\bar{g}(\lambda)$, where $\bar{b}(\lambda)$ and $\bar{g}(\lambda)$ are the appropriate CMFs and x is 0.0106 (1), 0.01625 (2) and 0.0087 (3). Open symbols: experimental data adjusted in macular and lens density for agreement with fundamentals. For details see text.

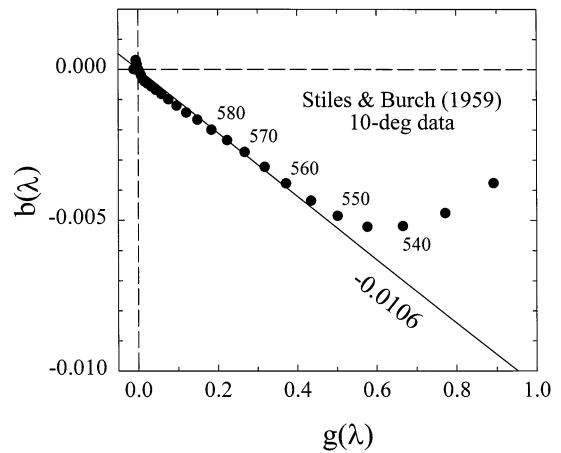


Fig. 10. Stiles and Burch (1959) 10 deg $g(\lambda)$ chromaticity coordinates plotted against the $b(\lambda)$ chromaticity coordinates (filled circles). The best-fitting straight line from 555 nm to long-wavelengths (continuous line) has a slope of -0.0106 .

Burch (1955). Function 3 is provided for those who want to retain the Smith and Pokorny (1975) L- and M-cone fundamentals, but would prefer to use a more plausible S-cone fundamental than the $\bar{z}(\lambda)$ CMF.

The details of the final derivations are as follows:

(1a,b) Stiles and Burch (1959) 10 deg CMFs. First, we determined the best-fitting ratio of $\bar{b}(\lambda)$ to $\bar{g}(\lambda)$ for the 10 deg CMFs using the method described above. Fig. 10 shows as filled circles the Stiles and Burch (1959) $g(\lambda)$ chromaticity coordinate plotted against the $b(\lambda)$ chromaticity coordinate at middle- and long-wavelengths. The slope of the best-fitting line (continuous line) ≥ 555 nm is -0.0106 . This implies that the relative S-cone spectral sensitivity is $\bar{b}(\lambda) + 0.0106\bar{g}(\lambda)$, which is similar to the function adopted by Stockman et al. (1993).

We then adjusted the $\bar{b}(\lambda) + 0.0106\bar{g}(\lambda)$ from 10 deg to 2 deg by assuming a photopigment optical density increase of 0.1 (from 0.3 to 0.4; within limits, the absolute densities are not critical in this calculation), and a macular density increase from a peak of 0.095 to one of 0.35. These values were based on analyses of the differences between the Stiles and Burch 2 deg and 10 deg CMFs, the differences between S-, M- and L-cone fundamentals derived from the two sets of CMFs and our data, and on calculations from the cone fundamentals back to photopigment spectra. The chosen values represent our ‘best guess’ based on all this information.

The 2 deg macular density of 0.35 is also based on 2 deg macular density estimates: 0.26 ($n = 5$) from this study; 0.32 ($n = 11$) from Stockman et al. (1993); 0.36 ($n = 9$) from Smith and Pokorny (1975); and 0.38 ($n = 38$) from (Sharpe, Stockman, Jägle, Knau, Klausen, Reitner et al., in press). Given the differences between the retinal distributions of the S-cones and the L- and M-cones (see above), we recognize that the effective

macular pigment density for the central 2 deg is probably lower for S-cone-mediated vision than for L- or M-cone-mediated vision. However, for simplicity, and because the relevant density values are uncertain, we assume similar densities. The $\bar{b}(\lambda) + 0.0106\bar{g}(\lambda)$ function after adjustment to 2 deg is shown as the filled circles in Fig. 9. We adopt this function as the S-cone fundamental from 390 to 510 nm, as indicated by the upper continuous line.

To produce the S-cone fundamental from 515 to 615 nm, we used both the CMF function and our experimental data. First, we adjusted our data in macular and lens density to be consistent with the filled circles in Fig. 9. An increase in lens density of 13% of the lens density spectrum of Table 3 and an increase of 0.06 in peak macular density were required. The adjusted experimental data are shown by the open circles. We then combined and smoothed our data from 510 to 615 nm and the CMF data from 510 to 540 nm by fitting a Gaussian function simultaneously to both sets of data (using a frequency rather than wavelength scale). The Gaussian function is shown by the upper continuous line from 515 to 615 nm. We tried many different types of function, before deciding on the Gaussian, which provides an excellent fit to our data and the CMFs over this range. We attach no special significance to the agreement between the Gaussian function and our data. The fits and function were generated by TableCurve 2D (Jandel). The CMF-based function and the experimental data were combined from 515 nm in order to smooth the slight bump in the CMF-based function at 520 nm (filled circles). The 2 deg function (1a) is tabulated in Table 3.

To calculate the 10 deg function (1b) tabulated in Table 3, we simply readjusted the 2 deg function back to 10 deg, using the same assumptions previously used to adjust the 10 deg function to 2 deg. From 390 to 510 nm, therefore, the 10 deg S-cone fundamental is exactly $\bar{b}(\lambda) + 0.0106\bar{g}(\lambda)$, where $\bar{b}(\lambda)$ and $\bar{g}(\lambda)$ are the Stiles and Burch (1959) 10 deg CMFs.

(2) Stiles and Burch (1955) 2 deg CMFs. We used the function $\bar{b}(\lambda) + 0.01625\bar{g}(\lambda)$ (filled diamonds, Fig. 9) to define S-cone spectral sensitivity from 390 to 520 nm (middle continuous line). The ratio of $\bar{b}(\lambda)$ to $\bar{g}(\lambda)$ is derived from the best-fitting slope (-0.01625) shown in Fig. 8d, but is almost identical to the linear combination ($\bar{b}(\lambda) + 0.01630\bar{g}(\lambda)$) that best fit the central data (see Fig. 7a).

We combined the function $\bar{b}(\lambda) + 0.01625\bar{g}(\lambda)$ with our experimental data to produce the S-cone fundamental from 525 to 615 nm. First, we adjusted our data in macular and lens density to be consistent with $\bar{b}(\lambda) + 0.01625\bar{g}(\lambda)$, requiring an increase in lens density of 9% of the lens density spectrum of Table 3 and an increase of 0.06 in peak macular density. The adjusted experimental data are shown by the open diamonds.

We then combined and smoothed our data from 510 to 615 nm and the CMF data from 510 to 560 nm again by fitting a Gaussian function simultaneously to both sets of data. The part of the Gaussian function used to define the fundamental is shown by the part of continuous line from 525 to 615 nm. The function (2) is tabulated in Table 3.

(3) Judd, Vos CIE 2 deg CMFs. We used the function $\bar{b}(\lambda) + 0.0087\bar{g}(\lambda)$ (filled squares, Fig. 9) to define S-cone spectral sensitivity from 390 to 565 nm (lower continuous line). The function is the linear combination of $\bar{b}(\lambda)$ and $\bar{g}(\lambda)$ that best fit the central data (see Fig. 7b), which we use in preference to the best-fitting slope (-0.0079) shown in Fig. 8a because of uncertainties surrounding the original data (see above).

We combined $\bar{b}(\lambda) + 0.0087\bar{g}(\lambda)$ with our experimental data to produce the S-cone fundamental from 570 to 615 nm. First, we adjusted our data in macular and lens density to be consistent with $\bar{b}(\lambda) + 0.0087\bar{g}(\lambda)$, which required an increase in lens density of 9% of the lens density spectrum of Table 3 and an increase of 0.42 in peak macular density. The adjusted experimental data are shown by the open squares. We then combined and smoothed our data from 510 to 615 nm and the CMF data from 510 to 565 nm by fitting a Gaussian function simultaneously to both sets of data. The part of the Gaussian function used to define the fundamental is shown by the middle continuous line from 570 to 615 nm. The function (3) is tabulated in Table 3.

5.1. Problems with the CIE 1964 10 deg CMFs

Unlike Stockman et al. (1993), we chose to leave the S-cone fundamental as a linear combination of the original Stiles and Burch 10 deg CMFs rather than ‘transforming’ them to the CIE 1964 10 deg CMFs. The CIE 1964 CMFs are based mainly on the 10 deg CMFs of Stiles and Burch (1959), and to a lesser extent on the 10 deg CMFs of Speranskaya (1959). While the CIE 1964 CMFs are similar to the 10 deg CMFs of Stiles and Burch, they differ, particularly in the case of $\bar{b}(\lambda)$, in ways that compromise their use as the basis for cone fundamentals. First, at short wavelengths, the CIE 1964 functions have been artificially extended to 360 nm, which is well beyond the limit of the color matches (392 nm) measured by Stiles and Burch (1959). While a straightforward extension could simply be ignored, the CIE chose to accommodate their extension by making small changes to the CMFs in the measured range. Although the changes are less than 0.1 log unit, they are nevertheless critical in the case of the S-cones, since they distort the shape of the underlying photopigment spectrum near its peak. (Stockman et al. (1993) circumvented this problem by adjusting the lens template.) Second, at middle wavelengths, large adjustments have been made to the blue CMF above 520 nm. These

changes mean that the CIE CMFs cannot be used to derive the S-cone fundamental by finding the ratio of $\bar{b}(\lambda)$ to $\bar{g}(\lambda)$ at middle- and long-wavelengths, as we were able to do with the Stiles & Burch functions, and furthermore that the CIE 1964 CMFs cannot be used to define the S-cone fundamental above 520 nm.

5.2. Other S-cone estimates based on transformations of the color matching functions

Most other S-cone estimates are transformations of either the CIE 1931 CMFs, and variants thereof, or the Stiles and Burch (1955) CMFs. As discussed above, the S-cone fundamental most favored by other workers in the CIE space is simply the $\bar{z}(\lambda)$ CMF, which is still used extensively for color computations. It is typically referred to as the Smith and Pokorny S-cone fundamental (Fig. 11, filled circles).

S-cone fundamentals based on the Stiles and Burch (1955) CMFs include $\bar{b}(\lambda) + 0.0196\bar{g}(\lambda)$ proposed by Estévez (1979), $\bar{b}(\lambda) + 0.0330\bar{g}(\lambda)$ proposed by Smith, Pokorny and Zaidi (1983), and $\bar{b}(\lambda) + 0.0220\bar{g}(\lambda) + 0.0008\bar{r}(\lambda)$ proposed by Vos, Estévez and Walraven (1990). In each case, the weight on the $\bar{g}(\lambda)$ CMF is too high, so that each function is: (i) too sensitive in the

range from 530 to 570 nm, and (ii) inconsistent with the $\bar{b}(\lambda)$ to $\bar{g}(\lambda)$ ratio of the color matching data (see above).

Stockman et al. (1993) proposed two 2 deg S-cone fundamentals: one in terms of the Stiles and Burch (1955) 2 deg CMFs ($\bar{b}(\lambda) + 0.0165\bar{g}(\lambda)$) and a second in terms of the CIE 1964 10 deg CMFs ($0.040557\bar{x}_{10}(\lambda) - 0.019683\bar{y}_{10}(\lambda) + 0.486195\bar{z}_{10}(\lambda)$) corrected to 2 deg. These functions were determined in part from a consideration of the ratio of $\bar{b}(\lambda)$ to $\bar{g}(\lambda)$ in the Stiles and Burch 2 deg and 10 deg color matching data (as above), and in part on the shape of the Stiles π_3 field spectral sensitivity at middle wavelengths. Their second solution based on the CIE 1964 CMFs is shown by the dashed lines in Fig. 11. It is indistinguishable from the Stiles and Burch 10 deg based function proposed here (continuous line), except at very short wavelengths and at wavelengths above 540 nm. At longer wavelengths, the Stockman et al. (1993) function overestimates sensitivity.

The possibility that the Stockman et al. (1993) function was too sensitive at long wavelengths was pointed out by Vos (personal communication). Based partly on the Lewis (1956) formula, which has no currently accepted basis², Vos suggested the extension shown by the dotted diamonds in Fig. 11. Our data, and hence our proposed S-cone fundamental, are consistent with the Vos proposal. For comparison, the Judd, Vos modified CIE $\bar{z}(\lambda)$ function, or Smith-Pokorny S-cone fundamental, is also shown in Fig. 11 as filled circles.

From a practical point of view, such as calculating the relative cone excitations caused by broad-band or narrow-band lights, the differences between the proposed function and the Stockman, MacLeod and Johnson function are largely trivial, since they are in a region in which the S-cone excitation is small. The main exception would be narrow-band middle- or long-wavelength lights of high enough intensity to excite the S-cones. In contrast, the differences between the proposed function and the CIE $\bar{z}(\lambda)$ function, which is the Smith and Pokorny S-cone fundamental could be substantial for many narrow-band and some broad-band lights.

5.3. Other S-cone spectral sensitivity estimates based on threshold measurements

Stiles' π_3 field sensitivity (Stiles, 1953) is the most likely of his three S-cone field sensitivities to be the

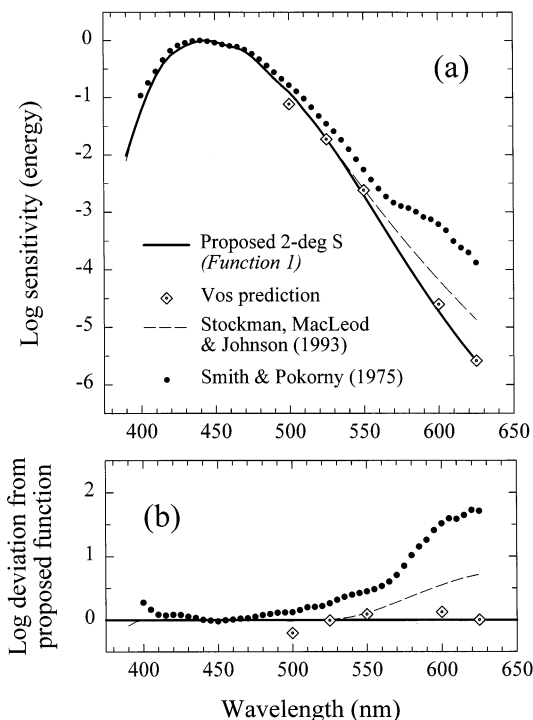


Fig. 11. (a) Comparison between the proposed S-cone spectral sensitivity function (continuous line), the Judd, Vos CIE $\bar{z}(\lambda)$ CMF or Smith-Pokorny S-cone fundamental (filled circles), and the Stockman et al. (1993) S-cone fundamental (dashed line). The extension suggested by Vos (personal communication) is shown by the dotted diamonds. (b) Differences between the proposed fundamental and the other functions.

² Lewis (1956) proposed an explanation of the common shape of the long-wave slope of all photopigments based on speculations about the number of vibrational modes of the chromophore group. His explanation, which now appears implausible, nevertheless does a surprisingly good job of defining the longer wavelength fall-off of the S-cone pigment.

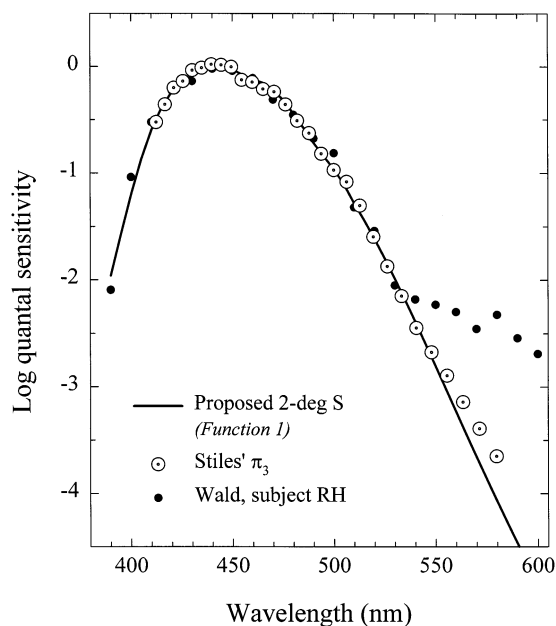


Fig. 12. Comparison between the proposed S-cone spectral sensitivity function (line), the π_3 field sensitivities of Stiles (open circles) from Wyszecki and Stiles (1982a), Table 2 (7.4.3), and the S-cone test sensitivities of Wald (1964) for subject RH (filled circles).

S-cone spectral sensitivity, since the field sensitivities of both π_1 and π_2 have secondary long-wavelength maxima that are uncharacteristic of single photopigments. Fig. 12 shows π_3 as dotted circles, and the proposed S-cone central spectral sensitivity estimate as the continuous line. The π_3 function has been adjusted in macular and lens density for consistency with the proposed S-cone fundamental, which required a decrease in lens density of 16% of the template of Table 3 and a decrease in peak macular density of 0.03.

The agreement between the proposed function and π_3 is good from short-wavelengths to 550 nm, which supports—if we only consider this range—the view of those (e.g. Pugh & Mollon, 1979) who argue that π_3 reflects the independent adaptation of the S-cones. Only at wavelengths greater than 555 nm, does π_3 start to deviate from the proposed function, which suggests that independent adaptation fails above 555 nm. As we argued above, since the field intensity required to raise the π_3 threshold grows rapidly with field wavelength, such a failure of independent adaptation (perhaps, even on metabolic grounds) becomes increasingly likely as the field wavelength increases and, relative to the S-cones, the M- and L-cones become more and more light adapted.

Also shown in Fig. 12 (filled circles) are the S-cone test sensitivities measured by Wald (1964) for subject RH. The Wald function has also been adjusted in macular and lens density for consistency with the proposed S-cone fundamental. In this case, a decrease in

lens density of 18% of the template of Table 3 and an increase in peak macular density of 0.30 were required. The agreement between Wald's data and the proposed function is also fairly good until 530 nm, after which the other cones take over target detection.

5.4. Pigment curves

The proposed S-cone spectral sensitivity should be consistent with direct measurements of individual S-cone photoreceptors, but, so far, few such measurements have been obtained in the human. One exception is Dartnall, Bowmaker and Mollon (1983), who used microspectrophotometry (MSP) to measure the photopigment absorption spectra of human S-cone photoreceptors. MSP is of little use in defining cone spectral sensitivities far away from the λ_{\max} , because of its poor signal to noise ratio. It can, however, be useful in determining the photopigment λ_{\max} . From their human MSP measurements Dartnall et al. (1983) estimate the human S-cone photopigment λ_{\max} to be 419.0 nm.

We estimated the λ_{\max} of the underlying S-cone photopigment from our mean spectral sensitivity data. First, we adjusted the central and peripheral data to the retinal level by removing the effects of a lens pigment with a density of 85% of the lens density spectrum of Table 3, and, for the central data, by removing the effects of a macular pigment with a peak density of 0.26 and the density spectrum Table 3. Last, we adjusted the spectrum to an infinitely low photopigment optical density from assumed peak axial photopigment densities of 0.43 and 0.20 for the central and peripheral measurements, respectively, and normalized them to unity peak (i.e. we calculated the normalized 'absorbance' spectrum). These values are based on the analysis of the original data (see above).

Once adjusted, we could estimate λ_{\max} by finding the wavelength at which the photopigment is most sensitive, but such a method is highly susceptible to experimental noise near the peak. A better method, which takes into account the shape of the whole curve, is to fit a theoretical 'standard' photopigment template shape, such as the one recently proposed by Lamb (1995), to the data.

Fig. 13 shows the adjusted central (a) and peripheral (b) data. The continuous curves are the Lamb photopigment templates for λ_{\max} values of 419.01 nm (a) and 418.72 nm (b). These values are best-fitting values. The agreement between the adjusted psychophysical data and the pigment templates is excellent, and is maintained over five or six decades of sensitivity. Such good agreement is remarkable, given that the only fitting parameter (apart from allowing a vertical shift) is λ_{\max} . Moreover, the λ_{\max} values that we obtain concur almost precisely with the MSP estimate.

The main difference between the central and peripheral measurements is that the latter agree with the Lamb template throughout the long-wavelength range, whereas the former show a slight loss of sensitivity beyond 585 nm. While it is tempting to dismiss the shortfall of the central data as experimental noise, it could reflect waveguide differences between the small central photoreceptors and the larger peripheral ones, which can, in principle, steepen the fall in sensitivity at longer wavelengths (see, for example, Enoch, 1961; Enoch & Stiles, 1961; Snyder, 1975; Horowitz, 1981).

Macaque S-cone spectral sensitivities have been estimated by suction electrode recordings (Baylor, Nunn & Schnapf, 1984), but the λ_{\max} of the macaque S-cone photopigment is longer than that of the human (Dartnall et al., 1983; Bowmaker, 1990; see Fig. 10 of Stockman et al., 1993). Thus, the suction electrode data cannot be directly compared with human data.

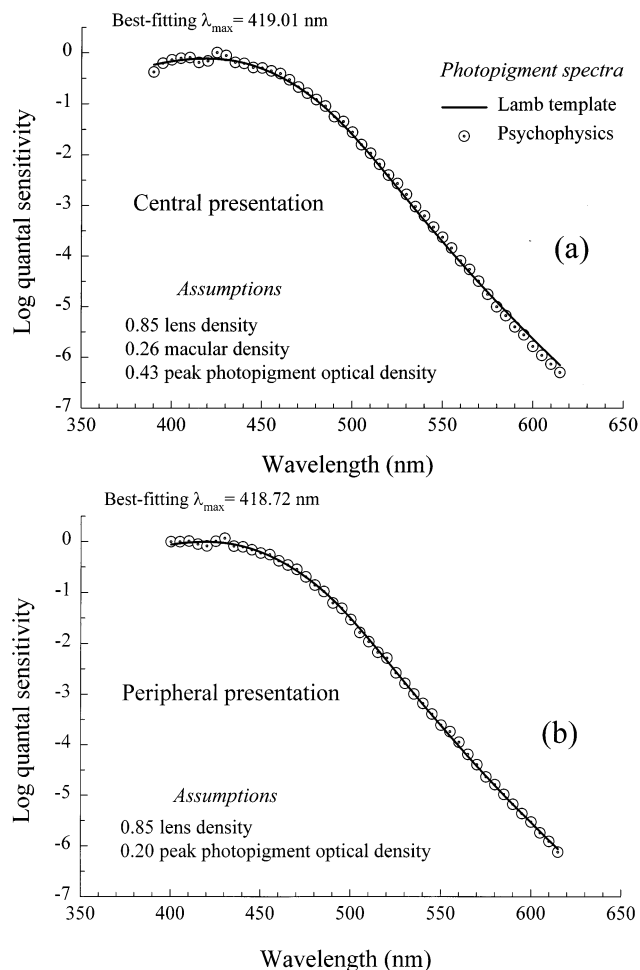


Fig. 13. The Lamb photopigment template (lines) fitted to the mean central (a) and peripheral (b) data after their adjustment to the retinal level and to low photopigment optical densities (circles). Best-fitting λ_{\max} values were 419.01 nm (a) and 418.72 nm (b).

5.5. Macular and photopigment densities

For normal observers, the change in S-cone photopigment optical density as presentation changes from the center to the periphery varies from 0.19 to 0.26 with a mean of 0.23. If, as in our analysis of the individual data, a fixed peak photopigment optical density of 0.20 is assumed at 13 deg in the periphery, then the peak optical density for normals in the central 2 deg varies from 0.39 to 0.46 with a mean of 0.43. (Equally, a peak of 0.10 could be assumed in the periphery, which would yield a mean value of 0.33 in the center.) Given the dangers of bleaching the S-cones with intense lights (see Harwerth & Sperling, 1975), there is understandably a lack of information about the optical density of the S-cones. Nor, unfortunately, do we have clear information about how the length of the human S-cone outer segment decreases with eccentricity. Ahnelt (private communication) suggests that, at the fovea, outer segments of S-cones may be 5% shorter than those of the M- and L-cones; whereas in the periphery, at retinal eccentricities greater than 5 mm (~ 18 deg of visual angle), they may be shorter by 15–20%. However, in the single electron micrographs showing outer segments, the histological study of Curcio et al. (1991, Fig. 3) indicates that, at a similar parafoveal location, the outer segment of an S-cone ($\sim 4.1 \mu\text{m}$) is almost 40% smaller than that of an L/M-cone ($7 \mu\text{m}$). A conservative interpretation of these values, assuming a density per unit length or specific absorbance of, say, $0.015 \mu\text{m}^{-1}$ (Bowmaker & Dartnall, 1980), suggests a change in optical pigment density between central foveal cones and peripheral cones of about 0.20 for the S-cones.

For the M- and L-cones, estimates of peak photopigment optical density obtained from bleaching experiments range from 0.27 to 0.60 (Terstiege, 1967; Miller, 1972; Smith & Pokorny, 1973; Alpern, 1979; Wyszecki & Stiles, 1982b; Burns & Elsner, 1993). Those based on the Stiles–Crawford effect are generally higher, ranging from 0.69 and 1.0 (Walraven, 1960; Enoch & Stiles, 1961), and are usually for a 1 deg field. Other estimates include ~ 0.5 from MSP (Bowmaker, Dartnall, Lythgoe & Mollon, 1978), if we assume a foveal cone outer segment length of $35 \mu\text{m}$ (Polyak, 1941). Retinal densitometry gives a peak photopigment optical density of 0.35 for the M-cones (Rushton, 1963), and 0.41 for the L-cones (King-Smith, 1973b,a). Thus, a peak S-cone optical density near 0.4 for normal, central vision lies well within the range of reported values for the M- and L-cones.

5.6. Other sources of variability

Some variability remains even after the individual data sets have been corrected to the same macular, photopigment and lens densities (see Fig. 5, above).

The remaining variability is likely to be due, in part, to experimental noise, and to errors in our density estimates. However, another potential source of variability is individual differences in the λ_{\max} of the S-cone photopigment.

To estimate λ_{\max} , we corrected the corneal spectral sensitivities to the retinal level using: (1) the lens density values tabulated in Column 2 of Table 1, assuming a mean density of 85% of the lens template; (2) the macular densities tabulated in Column 5 of Table 2, assuming a zero macular density for the peripheral data; and (3) the photopigment optical density differences tabulated in Column 6 of Table 2, assuming a fixed peak density for the peripheral data of 0.2. We then varied the λ_{\max} of the Lamb template to find the best-fitting template for both the central and peripheral data.

The mean central and peripheral λ_{\max} values were 416.9 nm (AS), 417.3 nm (LS), 417.6 nm (KS), 417.7 nm (PS), 419.7 nm (CF), 419.7 nm (FB), 420.5 nm (HJ) and 420.6 nm (TA). While the underlying variability in the S-cone λ_{\max} is probably continuous, there is a suggestion in our data of two clusters centered on 417.4 nm (AS, LS, KS and PS) and on 420.1 nm (CF, FB, HJ, TA). Although it may be purely coincidental, the implied amount of shift (2.7 nm) is reminiscent of that revealed by psychophysical investigations of the influence of the alanine/serine substitution at codon 180 in exon 3 of the X-chromosome-linked L- and M-cone photopigment genes (see, e.g. Sanocki, Lindsey, Winderickx, Teller, Deeb & Motulsky, 1993; He & Shevell, 1994; Sanocki, Shevell & Winderickx, 1994; Sharpe, Stockman, Jägle, Knau, Klausen, Reitner et al., in press).

5.7. Low photopigment densities with central presentation in blue monochromats

The simplest explanation for the low photopigment optical densities found with central presentation in blue-cone monochromats is that they fixate extrafoveally, where the cone outer segments are shorter than in the central fovea (e.g. Polyak, 1941). However, it is surprising that the photopigment optical densities for blue-cone monochromats with extrafoveal fixation are as low as they are for normals when the target is presented at 13 deg in the periphery. Perhaps, the S-cones in the rod-free area of the blue-cone monochromat, on which the centrally-presented target falls, tilt away from the optical axis because they are unsupported by surrounding photoreceptors. The effective optical density would then be lower, because light arriving from the pupil would travel transversely rather than longitudinally through the outer segment. Against this argument, however, is the finding that the Stiles–Crawford effect in blue-cone monochromats (Alpern et

al., 1971; Daw & Enoch, 1973) is comparable to that found in normals (Enoch & Stiles, 1961).

Acknowledgements

We are grateful to the subjects, who each worked for many hours on this project. We thank Richard Bone for providing the macular pigment density spectrum, which is tabulated in the Appendix, Sabine Aplitz for help and support, and Donald MacLeod and Françoise Viénot for comments. The work was supported by National Institutes of Health grant EY 10206 and National Science Foundation grant IBN 92-10046 awarded to co-author AS, and by the Deutsche Forschungsgemeinschaft (Bonn) grants SFB 325 Tp A13 and Sh23/5-1 and a Hermann- und Lilly-Schilling-Professur awarded to co-author LTS.

Appendix A

A.1. Proposed S-cone fundamental sensitivity curves

Table 3 lists the proposed S-cone fundamentals based on the Stiles and Burch (1959) 10 deg CMFs corrected to 2 deg (Column 2) and uncorrected (Column 3); the Stiles and Burch (1955) 2 deg CMFs (Column 4) and the 2 deg CIE 1931 CMFs corrected by Judd (1951) and Vos (1978) (Column 5). They are tabulated in quantal units. For further details, see above.

A.2. Lens and Macular pigment spectra

A.2.1. Macular pigment

The macular optical density spectrum is based on a spectrophotometer output curve provided by Bone (personal communication). It is tabulated in Table 3. The function appears in Fig. 3 of Bone, Landrum and Cains (1992), but only for wavelengths above 420 nm. Further details about its derivation can be found there. Briefly, the template was derived as follows: Lutein and zeaxanthin were mixed in the same ratio as found in the foveal region and incorporated into phospholipid membranes (in the form of liposomes). The absorbance spectrum of such liposome suspensions is grossly distorted by scattering, so a carotenoid-free liposome suspension has to be placed in the spectrophotometer reference cell. Bone et al. (1992) argue that this membrane environment more or less duplicates that of the carotenoids in the macula.

A.2.2. Lens pigment

As part of this study, we also derived a lens pigment density spectrum that is consistent with the proposed

Table 3

Wavelength (nm)	1a(2°): 2° S-cone based on the Stiles and Burch 10° CMFs Preferred	1b(10°): 10° S-cone based on the Stiles and Burch 10° CMFs Preferred	2: 2° S-cone based on the Stiles and Burch 2° CMFs	3: 2° S-cone based on the Judd, Vos modified CIE 2° CMFs	Lens: Proposed lens density spectrum	Macular: Macular density spectrum based on Bone et al.
390	-1.9642	-2.1515	-1.8598	-1.4828	2.5122	0.0453
395	-1.5726	-1.7425	-1.4570	-1.2024	2.1306	0.0649
400	-1.2020	-1.3528	-1.1604	-0.9454	1.7649	0.0868
405	-0.8726	-1.0031	-0.8415	-0.7290	1.4257	0.1120
410	-0.5986	-0.7098	-0.6091	-0.5337	1.1374	0.1365
415	-0.3899	-0.4812	-0.4163	-0.3379	0.9063	0.1631
420	-0.2411	-0.3067	-0.2573	-0.1797	0.7240	0.1981
425	-0.1526	-0.1921	-0.1455	-0.0938	0.5957	0.2345
430	-0.0821	-0.1032	-0.0858	-0.0511	0.4876	0.2618
435	-0.0356	-0.0477	-0.0401	-0.0241	0.4081	0.2772
440	-0.0004	-0.0068	-0.0126	-0.0190	0.3413	0.2884
445	-0.0051	0.0000	-0.0023	-0.0371	0.3000	0.3080
450	-0.0260	-0.0057	-0.0430	-0.0696	0.2629	0.3332
455	-0.0763	-0.0493	-0.0944	-0.1042	0.2438	0.3486
460	-0.1199	-0.0957	-0.1201	-0.1358	0.2279	0.3500
465	-0.1521	-0.1487	-0.1951	-0.1598	0.2131	0.3269
470	-0.2145	-0.2352	-0.2374	-0.2095	0.2046	0.2996
475	-0.3165	-0.3525	-0.3383	-0.2868	0.1929	0.2842
480	-0.4426	-0.4858	-0.4710	-0.3871	0.1834	0.2786
485	-0.5756	-0.6220	-0.6061	-0.5020	0.1749	0.2772
490	-0.7169	-0.7711	-0.7394	-0.6246	0.1675	0.2688
495	-0.8418	-0.9119	-0.8605	-0.7465	0.1601	0.2485
500	-0.9623	-1.0619	-0.9896	-0.8620	0.1537	0.2093
505	-1.1071	-1.2394	-1.1198	-0.9754	0.1463	0.1652
510	-1.2762	-1.4411	-1.2979	-1.1058	0.1378	0.1211
515	-1.4330	-1.6271	-1.4465	-1.2626	0.1293	0.0812
520	-1.6033	-1.8185	-1.6104	-1.4238	0.1230	0.0525
525	-1.7853	-2.0149	-1.7900	-1.5661	0.1166	0.0329
530	-1.9766	-2.2175	-1.9779	-1.7088	0.1102	0.0175
535	-2.1729	-2.4198	-2.1748	-1.8700	0.1049	0.0093
540	-2.3785	-2.6288	-2.3787	-2.0526	0.0986	0.0046
545	-2.5882	-2.8407	-2.5879	-2.2549	0.0922	0.0017
550	-2.8010	-3.0548	-2.8007	-2.4717	0.0859	0.0000
555	-3.0168	-3.2706	-3.0157	-2.7003	0.0795	0.0000
560	-3.2316	-3.4853	-3.2315	-2.9329	0.0742	0.0000
565	-3.4458	-3.6996	-3.4469	-3.1409	0.0678	0.0000
570	-3.6586	-3.9124	-3.6609	-3.3571	0.0615	0.0000
575	-3.8692	-4.1230	-3.8724	-3.5713	0.0551	0.0000
580	-4.0769	-4.3306	-4.0809	-3.7822	0.0488	0.0000
585	-4.2810	-4.5348	-4.2854	-3.9888	0.0435	0.0000
590	-4.4811	-4.7348	-4.4855	-4.1904	0.0381	0.0000
595	-4.6766	-4.9304	-4.6806	-4.3863	0.0329	0.0000
600	-4.8673	-5.1211	-4.8704	-4.5760	0.0297	0.0000
605	-5.0529	-5.3066	-5.0546	-4.7589	0.0254	0.0000
610	-5.2331	-5.4868	-5.2328	-4.9341	0.0223	0.0000
615	-5.4077	-5.6615	-5.4051	-5.1038	0.0191	0.0000

Proposed 2 and 10 deg S-cone fundamentals, lens pigment density spectrum, and the Bone macular density spectrum. The spectral sensitivities are in logarithmic quantal units, and are normalized to unity peak. The peaks are estimated to be approximately 441.1, 445.3, 443.5 and 438.6 nm, for the functions 1a, 1b, 2 and 3, respectively. The lens density is for a small pupil and is appropriate for Functions 1a and 1b. The lens densities from 620 to 660 nm are, in 5 nm steps: 0.0170, 0.0148, 0.0117, 0.0085, 0.0053, 0.0042, 0.0032, 0.0011, and 0.000, after which the densities are 0. The macular density spectrum is scaled to a density of 0.35 at 460 nm, which is the mean assumed density for 2 deg vision and is appropriate for Function 1a.

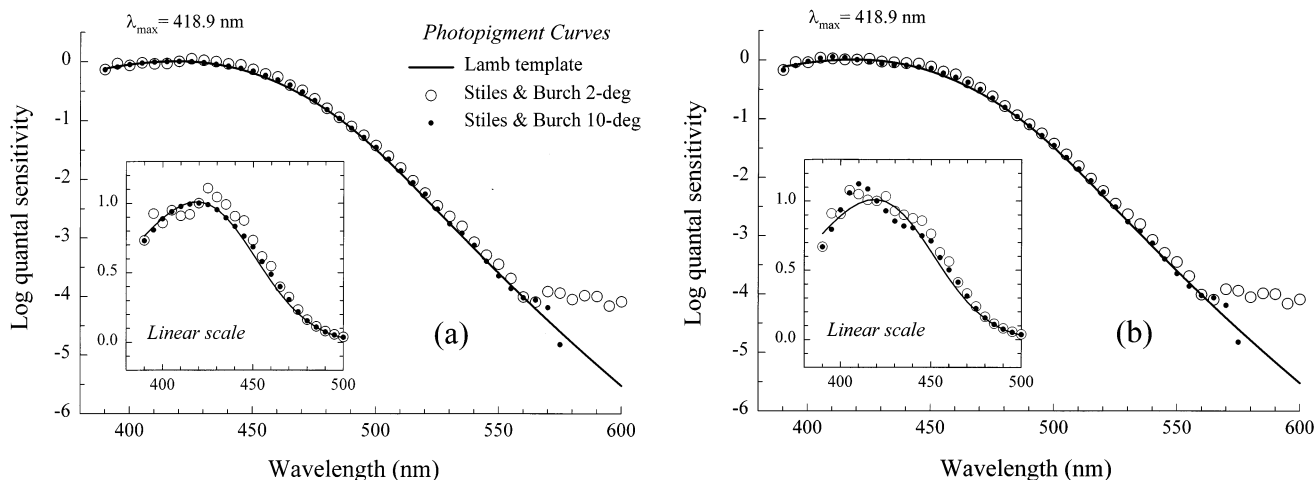


Fig. 14. S-cone fundamentals based solely on the Stiles and Burch (1959) 10 deg CMFs (filled circles) and the Stiles and Burch (1955) 2 deg CMFs (open circles) (i.e. before the incorporation of our data at middle wavelengths corrected to photopigment spectra using either (a) the proposed lens template (Column 5, Table 3) or (b) the lens template of van Norren and Vos (1974). The Lamb photopigment template is shown in both panels for a λ_{\max} of 418.9 (continuous lines). The lower left inset in each panel shows that data plotted against a linear ordinate.

S-cone fundamental based on the Stiles and Burch 10 deg CMFs. The need for such a derivation arose because existing lens pigment estimates did not yield smooth S-cone photopigment spectra when used to correct the corneal S-cone fundamentals (see Stockman et al., 1993). The effect of an existing lens template is shown in Fig. 14b, in which the S-cone functions $\bar{b}(\lambda) + 0.0106\bar{g}(\lambda)$, where $\bar{b}(\lambda)$ and $\bar{g}(\lambda)$ are the Stiles and Burch 10 deg CMFs, and $\bar{b}(\lambda) + 0.01625\bar{g}(\lambda)$, where $\bar{b}(\lambda)$ and $\bar{g}(\lambda)$ are the Stiles and Burch 2 deg CMFs, have been corrected to photopigment spectra using the van Norren and Vos lens template (1974). In making the corrections (and those shown in Fig. 14a), we assumed peak macular densities of 0.095 and 0.32 at 10 and 2 deg, respectively, peak axial photopigment optical densities of 0.3 and 0.4, and lens densities of 100 and 92.5% of the lens density spectrum in Table 3. Again, these are ‘best guesses’ based on a series of analyses. As can be seen more clearly in the inset, both photopigment spectra undulate around the λ_{\max} . As Stockman et al. (1993) pointed out, the undulations are probably due to a slight discrepancy in the lens pigment template near the S-cone λ_{\max} .

To overcome this problem, we propose the lens template tabulated in Table 3 and shown as the continuous line in Fig. 15a. It was obtained iteratively by correcting the van Norren and Vos template to produce the agreement between the 10 deg based photopigment spectrum (filled circles) and the Lamb template (continuous line) shown in Fig. 14a. Favoring the 10 deg function has inevitably left discrepancies between the 2 deg function (open circles) and the photopigment template. But the discrepancies are smaller than those obtained with the Stockman et al. (1993) lens template, which was derived in a similar way, but using the CIE

1964 10 deg CMFs. The template adopted by Stockman, MacLeod and Johnson, also incorporated the ‘adjustments’ made by CIE to the Stiles and Burch 10 deg CMFs, which are similar to the differences between

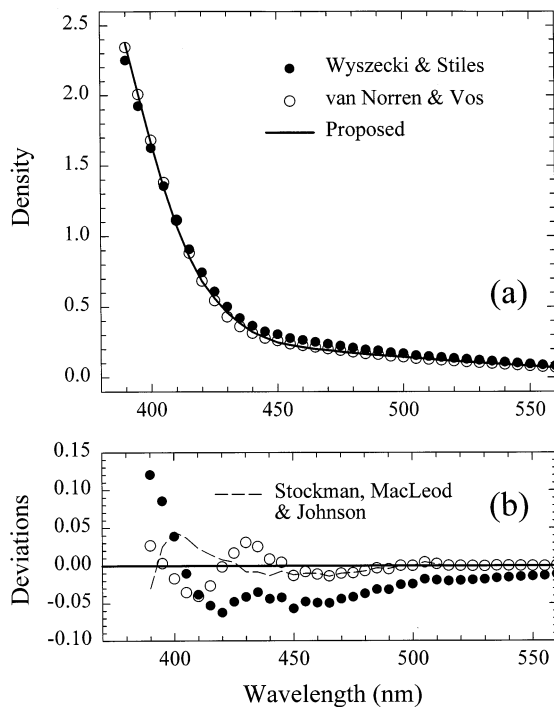


Fig. 15. (a) Comparison between the proposed lens density spectrum (continuous line), the van Norren and Vos (1974) spectrum (open circles), and the Wyszecki and Stiles (1982a) spectrum (filled circles). The proposed spectrum and the Wyszecki and Stiles spectrum have been adjusted in overall density to align with the van Norren and Vos spectrum. (b) Differences between the proposed spectrum and other functions. The difference between the proposed spectrum and the Stockman et al. (1993) spectrum is also shown (dashed line).

the Stockman, MacLeod and Johnson template and the proposed template shown as a dashed line in Fig. 15b.

Fig. 15b also shows the differences between the proposed template (continuous line) and the van Norren and Vos (1974) lens template (open circles) and the Wyszecki and Stiles (1982a) lens template (filled circles).

Although certainly dominated by lens pigment, the 'lens pigment' template tabulated in Table 3 is likely to reflect filtering by other things. Because of the way in which it was estimated, the template accounts for all those pigments or structures that alter spectral sensitivity and lie between the photoreceptor and the light arriving at the cornea. The same is true of many other lens pigment density estimates, including that of van Norren and Vos (1974), who compared the psychophysically-measured rod spectral sensitivity with the rhodopsin spectrum.

The data contained in Table 3 will be available on our Web sites: <http://www-cvrl.ucsd.edu> (America) and <http://www.eye.medizin.uni-tuebingen.de:81> (Germany).

References

- Ahnelt, P. K., Kolb, H., & Pflug, R. (1987). Identification of a subtype of cone photoreceptor, likely to be blue sensitive, in the human retina. *Journal of Comparative Neurology*.
- Alpern, A., Lee, G. B., & Spivey, B. E. (1965). π_1 cone monochromatism. *Archives of Ophthalmology*, 74, 334–337.
- Alpern, M. (1979). Lack of uniformity in colour matching. *Journal of Physiology*, 288, 85–105.
- Alpern, M., Lee, G. B., Maaseidvaag, F., & Miller, S. S. (1971). Colour vision in blue-cone 'monochromacy'. *Journal of Physiology*, 212, 211–233.
- Baylor, D. A., Nunn, B. J., & Schnapf, J. L. (1984). The photocurrent, noise and spectral sensitivity of rods of the monkey *Macaca fascicularis*. *Journal of Physiology*, 357, 575–607.
- Blackwell, H. R., & Blackwell, O. M. (1957). Blue mono-cone monochromacy: a new color vision defect. *Journal of the Optical Society of America*, 47, 338.
- Blackwell, H. R., & Blackwell, O. M. (1961). Rod and cone receptor mechanisms in typical and atypical congenital achromatopsia. *Vision Research*, 1, 62–107.
- Bone, R. A., Landrum, J. T., & Cains, A. (1992). Optical density spectra of the macular pigment in vivo and in vitro. *Vision Research*, 32, 105–110.
- Bone, R. A., Landrum, J. T., Fernandez, L., & Tarsis, S. L. (1988). Analysis of the macular pigment by HPLC: retinal distribution and age study. *Investigative Ophthalmology and Visual Science*, 29, 843–849.
- Bone, R. A., & Sparrock, J. M. B. (1971). Comparison of macular pigment densities in the human eye. *Vision Research*, 11, 1057–1064.
- Bongard, M. M., & Smirnov, M. S. (1954). Determination of the eye spectral sensitivity curves from spectral mixture curves. *Doklady Akademii nauk S.S.S.R.*, 102, 1111–1114.
- Bowmaker, J. K. (1990). Cone visual pigments in monkeys and humans. In N.R.C. Committee on Vision (Ed.), *Advances in photoreception: Proceedings of a symposium on the frontiers of visual science*. Washington, DC: National Academy Press.
- Bowmaker, J. K., & Dartnall, H. J. A. (1980). Visual pigments of rods and cones in the human retina. *Journal of Physiology*, 298, 501–512.
- Bowmaker, J. K., Dartnall, H. J. A., Lythgoe, J. N., & Mollon, J. D. (1978). The visual pigments of rods and cones in the rhesus monkey *Macaca mulatta*. *Journal of Physiology*, 274, 329–348.
- Brindley, G. S. (1954). The summation areas of human colour-receptive mechanisms at increment threshold. *Journal of Physiology*, 124, 400–408.
- Brindley, G. S., Du Croz, J. J., & Rushton, W. A. H. (1966). The flicker fusion frequency of the blue-sensitive mechanism of colour vision. *Journal of Physiology*, 183, 497–500.
- Burns, S. A., & Elsner, A. E. (1993). Color matching at high luminances: photopigment optical density and pupil entry. *Journal of the Optical Society of America A*, 10, 221–230.
- Castano, J. A., & Sperling, H. (1982). Sensitivity of the blue-sensitive cones across the retina. *Vision Research*, 22, 661–673.
- Curcio, C. A., Allen, K. A., Sloan, K. R., Lerea, C. L., Hurley, J. B., Klock, I. B., & Milam, A. H. (1991). Distribution and morphology of human cone photoreceptors stained with anti-blue opsin. *Journal of Comparative Neurology*, 312, 610–624.
- Dartnall, H. J. A., Bowmaker, J. K., & Mollon, J. D. (1983). Human visual pigments: microspectrophotometric results from the eyes of seven persons. *Proceedings of the Royal Society of London, B220*, 115–130.
- Daw, N. W., & Enoch, J. M. (1973). Contrast sensitivity, Westheimer function and Stiles–Crawford effect in a blue cone monochromat. *Vision Research*, 13, 1669–1680.
- Eisner, A., & MacLeod, D. I. A. (1980). Blue sensitive cones do not contribute to luminance. *Journal of the Optical Society of America*, 70, 121–123.
- Enoch, J. M. (1961). Nature of the transmission of energy in the retinal receptors. *Journal of the Optical Society of America*, 51, 1122–1126.
- Enoch, J. M., & Stiles, W. S. (1961). The colour change of monochromatic light with retinal angle of incidence. *Optica Acta*, 8, 329–358.
- Estevez, O. (1979). *On the fundamental database of normal and dichromatic color vision*. Ph.D. thesis, Amsterdam University.
- Falls, H. F. (1960). Discussion following paper by Alpern, Falls and Lee. *American Journal of Ophthalmology*, 50, 1012.
- Green, D. G. (1968). The contrast sensitivity of the colour mechanisms of the human eye. *Journal of Physiology*, 196, 415–429.
- Grutzner, P. (1964). Der normale Farbensinn und seine abweichungen. *Bericht der Deutschen ophthalmologischen Gesellschaft*, 66, 161–172.
- Guild, J. (1931). The colorimetric properties of the spectrum. *Philosophical Transactions of the Royal Society of London, A230*, 149–187.
- Harwerth, R. S., & Sperling, H. G. (1975). Effects of intense visible radiation on the increment threshold spectral sensitivity of the Rhesus monkey eye. *Vision Research*, 15, 1193–1204.
- He, J. C., & Shevell, S. K. (1994). Individual differences in cone photopigments of normal trichromats measured by dual Rayleigh-type color matches. *Vision Research*, 34, 367–376.
- Hess, R. F., Mullen, K. T., Sharpe, L. T., & Zrenner, E. (1989). The photoreceptors in atypical achromatopsia. *Journal of Physiology*, 417, 123–149.
- Horowitz, B.R. (1981). Theoretical considerations of the retinal receptor as a waveguide. In J.M. Enoch & F.L. Tobey (Eds.), *Vertebrate photoreceptor optics* (pp. 217–300). Berlin, New York: Springer-Verlag.
- Judd, D.B. (1951). Report of U.S. Secretariat Committee on Colorimetry and Artificial Daylight. *Proceedings of the Twelfth Session of the CIE, Stockholm* (pp. 11). Paris: Bureau Central de la CIE.
- Kelly, D. H. (1974). Spatio-temporal frequency characteristics of color-vision mechanisms. *Journal of the Optical Society of America*, 64, 983–990.

- King-Smith, P. E. (1973a). The optical density of erythrolabe determined by a new method. *Journal of Physiology*, 230, 551–560.
- King-Smith, P. E. (1973b). The optical density of erythrolabe determined by retinal densitometry using the selfscreening method. *Journal of Physiology*, 230, 535–549.
- Knowles, A., & Dartnall, H. J. A. (1977). The photobiology of vision. In H. Davson (Ed.), *The Eye, Vol 2B*. London: Academic.
- Lamb, T. D. (1995). Photoreceptor spectral sensitivities: common shape in the long-wavelength spectral region. *Vision Research*, 35, 3083–3091.
- Lewis, P. R. (1956). A theoretical interpretation of spectral sensitivity curves at long wavelengths. *Journal of Physiology*, 130, 45–52.
- Miller, S. S. (1972). Psychophysical estimates of visual pigment densities in red-green dichromats. *Journal of Physiology*, 223, 89–107.
- Mollon, J. D. (1982). Color Vision. *Annual Review of Psychology*, 33, 41–85.
- Nathans, J., Davenport, C. M., Maunee, I. H., Lewis, R. A., Hejtmancik, J. F., Litt, M., Lovrien, E., Weleber, R., Bachynski, B., Zwas, F., Klingaman, R., & Fishman, G. (1989). Molecular genetics of human blue cone monochromacy. *Science*, 245, 831–838.
- Nathans, J., Maunee, I. H., Zrenner, E., Sadowski, B., Sharpe, L. T., Lewis, R. A., Hansen, E., Rosenberg, T., Schwartz, M., Heckenlively, J. R., Traboulsi, E., Klingaman, R., Bech-Hansen, N. T., LaRoche, G. R., Pagon, R. A., Murphey, W. H., & Weleber, R. G. (1993). Genetic heterogeneity among blue-cone monochromats. *American Journal of Human Genetics*, 53, 987–1000.
- Pease, P. L., Adams, A. J., & Nuccio, E. (1987). Optical density of human macular pigment. *Vision Research*, 27, 705–710.
- Pokorny, J., Smith, V. C., & Swartley, R. (1970). Threshold measurements of spectral sensitivity in a blue cone monochromat. *Investigative Ophthalmology and Visual Science*, 9, 807–813.
- Polyak, S.L. (1941). *The Retina*. Chicago: University of Chicago.
- Pugh, E. N., & Mollon, J. D. (1979). A theory of the π_1 and π_3 color mechanisms of Stiles. *Vision Research*, 20, 779–788.
- Reitner, A., Sharpe, L. T., & Zrenner, E. (1991). Is colour vision possible with only rods and blue-sensitive cones? *Nature*, 352, 798–800.
- Ruddock, K. H. (1965). The effect of age upon colour vision II. Changes with age in light transmission of the ocular media. *Vision Research*, 5, 47–58.
- Rushton, W. A. H. (1963). The density of chlorolabe in the foveal cones of a protanope. *Journal of Physiology*, 168, 360–373.
- Sanocki, E., Lindsey, D. T., Winderickx, J., Teller, D. Y., Deeb, S. S., & Motulsky, A. G. (1993). Serine/alanine amino acid polymorphism of the L and M-cone pigments: Effects on Rayleigh matches among deuteranopes, protanopes and color normal observers. *Vision Research*, 33, 2139–2152.
- Sanocki, E., Shevell, S. K., & Winderickx, J. (1994). Serine/alanine amino acid polymorphism of the L-cone photopigment assessed by dual Rayleigh-type color matches. *Vision Research*, 34, 377–382.
- Sharpe, L. T., Fach, C. C., & Stockman, A. (1992). The field adaptation of the human rod visual system. *Journal of Physiology*, 445, 319–343.
- Sharpe, L.T., Stockman, A., Jägle, H., Knau, H., Klausen, G., Reitner, A., & Nathans, J. Red, green, and red–green hybrid photopigments in the human retina: correlations between deduced protein sequences and psychophysically-measured spectral sensitivities. *Journal of Neuroscience* (in press).
- Smith, V. C., & Pokorny, J. (1973). Psychophysical estimates of optical density in human cones. *Vision Research*, 13, 1199–1202.
- Smith, V. C., & Pokorny, J. (1975). Spectral sensitivity of the foveal cone photopigments between 400 and 500 nm. *Vision Research*, 15, 161–171.
- Smith, V. C., Pokorny, J., Delleman, J. W., Cozijnsen, M., Houtman, W. A., & Went, L. N. (1983). X-linked incomplete achromatopsia with more than one class of functional cones. *Investigative Ophthalmology and Visual Science*, 24, 451–457.
- Smith, V.C., Pokorny, J., & Zaidi, Q. (1983). How do sets of Color-Matching Functions differ? In J.D. Mollon & L.T. Sharpe (Eds.), *Colour Vision: Physiology and Psychophysics*. London: Academic.
- Snyder, A.W. (1975). Photoreceptor optics-theoretical principles. In A.W. Snyder & R. Menzel (Eds.), *Photoreceptor optics* (pp. 38–55). Berlin: Springer-Verlag.
- Speranskaya, N. I. (1959). Determination of spectrum color co-ordinates for twenty-seven normal observers. *Optics and Spectroscopy*, 7, 424–428.
- Sperling, H.G. (1958). An experimental investigation of the relationship between colour mixture and luminous efficiency, *Visual Problems of Colour, Volume 1* (pp. 249–277). London: Her Majesty's Stationery Office.
- Spivey, B. E. (1965). The X-linked recessive inheritance of atypical monochromatism. *Archives of Ophthalmology*, 74, 327–333.
- Stiles, W. S. (1939). The directional sensitivity of the retina and the spectral sensitivity of the rods and cones. *Proceedings of the Royal Society of London, B127*, 64–105.
- Stiles, W. S. (1946). Separation of the 'blue' and 'green' mechanisms of foveal vision by measurements of increment thresholds. *Proceedings of the Royal Society of London, B*, 133, 418–434.
- Stiles, W. S. (1949). Incremental thresholds and the mechanisms of colour vision. *Documenta Ophthalmologica*, 3, 138–163.
- Stiles, W. S. (1953). Further studies of visual mechanisms by the two-colour threshold technique. *Coloquio sobre problemas opticos de la vision*, 1, 65–103.
- Stiles, W. S. (1959). Color vision: the approach through increment threshold sensitivity. *Proceedings of the National Academy of Science USA*, 45, 100–114.
- Stiles, W. S. (1964). Foveal threshold sensitivity on fields of different colors. *Science*, 145, 1016–1018.
- Stiles, W.S. (1978). *Mechanisms of Colour Vision*. London: Academic.
- Stiles, W.S., & Burch, J.M. (1955). Interim report to the Commission Internationale de l'Eclairage Zurich, 1955, on the National Physical Laboratory's investigation of colour-matching (1955) with an appendix by W.S. Stiles & J.M. Burch. *Optica Acta*, 2, 168–181.
- Stiles, W. S., & Burch, J. M. (1959). NPL colour-matching investigation: Final report (1958). *Optica Acta*, 6, 126.
- Stockman, A., MacLeod, D. I. A., & DePriest, D. D. (1991). The temporal properties of the human short-wave photoreceptors and their associated pathways. *Vision Research*, 31, 189–208.
- Stockman, A., MacLeod, D. I. A., & Johnson, N. E. (1993). Spectral sensitivities of the human cones. *Journal of the Optical Society of America A*, 10, 2491–2521.
- Stockman, A., & Sharpe, L.T. (1998). Human cone spectral sensitivities: a progress report. *Vision Research*, 38, 3193–3206.
- Terstiege, H. (1967). Untersuchungen zum Persistenz- und Koeffizientensatz. *Die Farbe*, 16, 1–120.
- van Norren, D., & Vos, J. J. (1974). Spectral transmission of the human ocular media. *Vision Research*, 14, 1237–1244.
- Vos, J.J. (1972). *Literature review of human macular absorption in the visible and its consequences for the cone receptor primaries*. Soesterberg, The Netherlands: Netherlands Organization for applied scientific research, Institute for Perception.
- Vos, J. J. (1978). Colorimetric and photometric properties of a 2-deg fundamental observer. *Color Research and Application*, 3, 125–128.
- Vos, J. J., Estévez, O., & Walraven, P. L. (1990). Improved color fundamentals offer a new view on photometric additivity. *Vision Research*, 30, 936–943.
- Vos, J. J., & Walraven, P. L. (1971). On the derivation of the foveal receptor primaries. *Vision Research*, 11, 799–818.

- Wald, G. (1945). Human vision and the spectrum. *Science*, *101*, 653–658.
- Wald, G. (1964). The receptors of human color vision. *Science*, *145*, 1007–1016.
- Wald, G. (1967). Blue-blindness in the normal fovea. *Journal of the Optical Society of America*, *57*, 1289–1301.
- Walraven, P. L. (1960). On the Bezold-Brücke phenomenon. *Journal of the Optical Society of America*, *51*, 1113–1116.
- Williams, D. R., MacLeod, D. I. A., & Hayhoe, M. M. (1981). Foveal Tritanopia. *Vision Research*, *19*, 1341–1356.
- Wright, W. D. (1928). A re-determination of the trichromatic coefficients of the spectral colours. *Transactions of the Optical Society*, *30*, 141–164.
- Wyszecki, G., & Stiles, W. S. (1967). *Color Science: concepts and methods, quantitative data and formulae* (1st ed.). New York: Wiley.
- Wyszecki, G., & Stiles, W. S. (1982a). *Color Science: concepts and methods, quantitative data and formulae* (2nd ed.). New York: Wiley.
- Wyszecki, G., & Stiles, W. S. (1982b). High-level trichromatic color matching and the pigment-bleaching hypothesis. *Vision Research*, *20*, 23–37.
- Zrenner, E., Magnussen, S., & Lorenz, B. (1988). Blauzapfenmonochromasie: Diagnose, genetische Beratung und optische Hilfsmittel. *Klinische Monatsblätter für Augenheilkunde*, *193*, 510–517.